LipoParticles: A Lipid Membrane Coating onto Polymer Particles to Enhance the Internalization in Osteoblast Cells

Florian Vanneste, Allison Faure, Mathieu Varache, Mario Menendez-Miranda, Virginie Dyon-Tafani, Sébastien Dussurgey, Elisabeth Errazuriz-Cerda, Veronica La Padula, Pierre Alcouffe, Marie Carrière, et al.

LipoParticles: A Lipid Membrane Coating onto Polymer Particles to Enhance the Internalization in Osteoblast Cells

Florian Vanneste[a], Allison Faure[b], Mathieu Varache[a], Mario Menendez-Miranda[c], Virginie Dyon-Tafani[b], Sébastien Dussurgey[d], Elisabeth Errazuriz-Cerda[e], Veronica La Padula[f], Pierre Alcouffe[a], Marie Carrière[g], Ruxandra Gref[c], Frédéric Laurent[b], Jérôme Josse[b,*], Catherine Ladavière[a,*]

[a]. Université de Lyon, CNRS, Université Claude Bernard Lyon 1, INSA Lyon, Université Jean Monnet, UMR 5223, Ingénierie des Matériaux Polymères F-69622 Cedex, France

[b]. Centre International de Recherche en Infectiologie (CIRI), Université de Lyon, Inserm, U1111, Université Claude Bernard Lyon 1, CNRS, UMR5308, ENS de Lyon, Lyon, France

[c]. Institut de Sciences Moléculaires d'Orsay (ISMO), Univ.of Paris-Sud, Orsay 91405, France

[d]. Structure Fédérative de Recherche Biosciences, UMS344/US8, Inserm, CNRS, Université Claude Bernard Lyon-1, ENS de Lyon, Lyon, France.

[e]. Centre d'Imagerie Quantitative Lyon-Est (CIQLE), Université Claude Bernard Lyon 1, Lyon, France.

[f]. Centre Technologique des Microstructures, Université Claude Bernard Lyon 1, Villeurbanne, France.

[g]. Université Grenoble-Alpes, CEA, CNRS, IRIG, SyMMES, CIBEST, 38000 Grenoble, France.

*Corresponding authors:

orcid.org/0000-0001-6780-9646. Email: jerome.josse@univ-lyon1.fr

orcid.org/0000-0002-6039-7471. Email: catherine.ladaviere@univ-lyon1.fr

Abstract

LipoParticles, core-shell assemblies constituted of a polymer core coated by a lipid membrane, are promising carriers for drug delivery applications with intracellular targets. This is of a great interest since it is actually challenging to treat infections involving intracellular bacteria such as bone and joint ones for which the bacteria are hidden in osteoblast cells. The present work reports for the first time to the better of our knowledge the proof of an enhanced internalization of particles in osteoblast cells thanks to a lipid coating of particles (= LipoParticles). The *ca* 300 nm-sized assemblies were elaborated by reorganization of liposomes (composed of DPPC/DPTAP 10/90 mol./mol.) onto the surface of poly(lactic-*co*-glycolic acid) (PLGA) particles, and were characterized by dynamic light scattering (DLS), transmission electron microscopy (TEM), and zetametry. An optimization of these assemblies was also performed by adding poly(ethylene glycol) (PEG) chains on their surface (corresponding to a final formulation of DPPC/DPTAP/DPPE-PEG5000 8/90/2 mol./mol./mol.). Interestingly, this has provided them a colloidal stability after their 20-fold dilution in PBS or cell culture medium, and made possible their freeze-drying without forming aggregates after their re-hydration. Their non-cytotoxicity towards a human osteoblast cell line (MG63) was also demonstrated. The enhanced internalization of LipoParticles in this MG63 cell line, in comparison with PLGA particles, was proven by observations with a confocal laser scanning microscope, as well as by flow cytometry assays. Finally, this efficient internalization of LipoParticles in MG63 cells was confirmed by TEM on ultrathin sections, which has also revealed a localization close to intracellular *Staphylococcus aureus*.

Highlights (below to 80 words)

- Elaboration and characterization of LipoParticles constituted of PLGA particles coated with a lipid membrane.
- Optimization of their lipid formulation with PEG chains for a better colloidal stability in biological media, and a non-aggregating freeze-drying.
- Proofs of their non-cytotoxicity towards a human osteoblast cell line (MG63), and an enhanced internalization of LipoParticles in MG63 cells, *versus* PLGA particles, by CLSM, and flow cytometry assays.
- Observation of their internalization in MG63 cells infected by intracellular *Staphylococcus aureus* by TEM on ultrathin sections.

Keywords

LipoParticles; Liposomes; Lipid membranes; PLGA particles; Osteoblast internalization; Drug delivery systems

Introduction

Bone and joint infections (BJIs), especially the ones associated with prosthesis, are a major Public Health problem. Indeed, with the aging of the population, the number of arthroplasties continues to grow, inevitably increasing the number of BJIs. Staphylococci, and particularly *Staphylococcus aureus*, are the most prevalent pathogens in BJIs. This bacterium can develop antibiotic resistances, complexifying the management of these infections. Moreover, even with appropriate medical and surgical management and optimal antibiotic treatment, *Staphylococcus aureus* can persist in the periprosthetic tissues, leading to the chronicization of BJIs or to relapsing infections[1].

Long regarded as an extracellular pathogen, *Staphylococcus aureus* can be internalized by host cells such as macrophages or neutrophils, as well as non-professional phagocytic cells such as epithelial cells, endothelial cells, fibroblasts, or osteoblasts. In the context of BJIs, *Staphylococcus aureus* can survive intracellularly inside osteoblasts (the bone forming cells), and is thus protected from the activity of most of the antibiotics and from immune system[2, 3].

New antibiotics are regularly discovered and developed to fight staphylococcal infections[4]. However, in the specific context of intracellular *Staphylococcus aureus*, the ability of antibiotics to cross through the host cell membrane to attain the intracellular localization is still an important issue that could explain the high rate of relapse in staphylococcal BJIs.

Nanotechnology-based species, such as liposomes and polymer particles, have emerged as new drug delivery systems to circumvent the limitations of traditional medicine[5]. Some of these drug delivery systems have been approved by the FDA, and have even reached a clinical use[6, 7].

Liposomes have extensively been valorized for the delivery of drugs, for instance in treatments of cancer, as well as fungal, viral, and bacterial infections[8, 9, 10]. Indeed, the particular physicochemical behavior of liposomes such as their possible encapsulation of

hydrophilic, lipophilic, and amphiphilic drugs can explain their use as drug delivery systems. Moreover, liposomes present satisfactory biocompatibility and bioresorbability, increase the drug bioavaibility, and decrease drug toxicity thanks to their encapsulation inside liposomes. Unfortunately, the liposomes can also show a low colloidal stability, and a short half-life in human body. Furthermore, encapsulated drugs can possibly leak from liposomes during their vectorization towards their target.

Polymer particles have many advantages such as a size distribution which can be narrow, a controlled size, and reproducible and scalable elaboration processes[11]. Moreover, their surface can be modified by ligands to obtain a drug vectorization towards targeted pathologic area[12]. Poly(lactic-*co*-glycolic acid) (PLGA), which is biocompatible, bioresorbable, with a FDA-approved utilization, is one of the best polymer candidates for the elaboration as drug delivery systems[13, 14, 15, 16, 17].

In order to put together these well-known advantages of liposomes and polymer particles in drug delivery applications, their assembly, corresponding to polymer particles coated with a lipid membrane, has been developed. They are named in the literature: "LipoParticles"[18, 19, 20, 21, 22, 23, 24, 25, 26, 27, 28, 29], "lipid-coated nanoparticles"[30], "nanocell"[31], "polymer-supported lipid shells"[32], "lipid-enveloped hybrid nanoparticles"[33], "lipid-polymer hybrid nanoparticles"[34], or "lipid-coated polymeric nanoparticles"[35]. This lipid surface modification of particles affords several interesting advantages to the assemblies such as a better control of the drug release not only because of the degradation of their polymer core tridimensional matrix, but also the diffusional barrier constituted by their lipid envelope[36, 37]. Moreover, the lipid surface can easily be modified, for instance, with poly(ethylene glycol) (PEG) chains, and/or ligands in order to produce stealth assemblies, and/or assemblies showing an active vectorization process as already demonstrated for the liposomes[38, 39]. Finally, the polymer core can contribute to the structural stability of resulting assemblies in comparison with

liposomes, while the lipid coating provides them an external biomimetic behavior, and a modulated/tuned surface function. These core-shell assemblies have already been elaborated with synthetic polymer (*e.g.*, poly(lactic acid)[19, 20, 40, 41], PLGA[42, 43], and polystyrene[21, 22, 24]) and MOF[44] cores, and examined by electron microscopy[19, 20, 21, 32, 45].

However, interactions between these assemblies and cells have been poorly investigated in the literature. Their use has been reported for cancer applications[46, 47, 48]. Jadon *et al.*[46] have notably highlighted the benefits to use these assemblies as nanovectors for the release of drugs inside cells *versus* free drugs. Indeed, *in vitro* cell studies have shown a greater cellular uptake of docetaxel (DTX) at lower IC 50 in breast cancer cell lines. Moreover, *in vivo* studies have exhibited better pharmacokinetics, and a tumor targetability with DTX-loaded assemblies as compared to free DTX, with the least drug distribution in various organs. Moreover, a noticeable percentage reduction in tumor burden was observed with these DTX-loaded assemblies in comparison with free DTX.

To resume, the use of these assemblies may allow the cell interaction to be improved, and the drug concentration to be increased in the cells. Nevertheless, to the better of our knowledge, there is no comparison in the literature between these assemblies and the corresponding polymer particles (*i.e.*, without a lipid coating) for this cell interaction.

In a effort to reach the intracellular compartment for the treatment of bone and joint pathologies, particles of PLGA, chitosan, or silica have been studied as nanocarriers to improve the internalization in osteoblast or pre-osteoblast cells[49, 50, 51, 52, 53, 54]. These studies have shown the possibility to deliver antibacterial drugs directly in these cells. Nevertheless, to the better of our knowledge, no work has been reported in the literature on the uptake of core-shell assemblies, that will be named here LipoParticles, in osteoblast cells in comparison with corresponding polymer particles.

Therefore, the main goals of the work described herein are to elaborate and characterize LipoParticles based on PLGA particles, as well as to study their uptake in osteoblast cells in comparison with bare PLGA particles. More precisely, the potential interest of a lipid coating onto PLGA particles on the uptake of resulting LipoParticles in a human osteoblast cell line (MG63) is examined by observations with a confocal laser scanning microscope, and a transmission electron microscope (TEM) on ultrathin sections, as well as by flow cytometry assays. Furthermore, studies of colloidal stability of these LipoParticles after their dilution in PBS or cell culture medium, their capacity of being freeze-dried, and their cytotoxicity towards the MG63 human osteoblast cell line complete these investigations in order to define if these core-shell assemblies could be interesting nanovectors to deliver antibiotics against intracellular *Staphylococcus aureus.*

Experimental Section

Materials and Methods

Materials

Zwitterionic 1,2-dipalmitoyl-*sn*-glycero-3-phosphocholine (DPPC, $C_{40}H_{80}NO_8P$) lipid, cationic 1,2-dipalmitoyl-3-trimethylammonium propane (DPTAP, $C_{38}H_{76}NO_4Cl$) lipid, fluorescent 1-palmitoyl-2-(dipyrromethene boron difluoride) undecanoyl-*sn*-glycero-3-phosphocholine (TopFluor®-PC, $C_{48}H_{83}BF_2N_3O_8P$) lipid, and 1,2-dipalmitoyl-*sn*-glycero-3-phosphoethanolamine-*N*-[methoxy(polyethylene glycol)-5000] (DPPE-PEG5000, $C_{265}H_{531}NO_{123}P$) polymer-lipid conjugate were obtained from Avanti Polar Lipids Inc. (Alabaster, AL). All lipids were used without further purification. The biodegradable PLGA (50/50) copolymer Expansorb® P019 wit an acid end-group was purchased from Sigma Aldrich. Polyvinyl alcohol (PVA) (88% hydrolyzed), and dichloromethane (DCM) were

purchased from Sigma-Aldrich (Saint-Quentin-Fallavier, France). The human osteoblast cell line used was MG63, CRL-1427, from LGC Standards, USA. For infection experiments, the well-characterized reference strain *Staphylococcus aureus* SH1000 was used.

Methods

Elaboration of cationic liposomes

Liposomes were formulated according to the Bangham method[55]. This has consisted to dissolve lipids in chloroform with a specified ratio molar of DPPC/DPTAP 10/90 or DPPC/DPTAP/DPPE-PEG5000 8/90/2. For the confocal microscopy observations, a fluorescent lipid (TopFluor®-PC) was added to lipid formulations, and final molar ratios of DPPC/DPTAP/TopFluor®-PC 9/90/1 or DPPC/DPTAP/DPPE-PEG5000/TopFluor®-PC 7/90/2/1 were employed. Then, the solvent was removed by rotary evaporation to get a homogenous, and thin lipid film. Multilamellar vesicles (MLV) were obtained by adding an aqueous solution to this lipid film (resulting in a final lipid concentration of 10 mM), and by stirring this mixture at 60°C. Finally, a dispersion of small unilamellar vesicles (SUV) was obtained by extruding 11 times the obtained MLV dispersion through a calibrated polycarbonate membrane with a pore diameter of 100 nm for the formulation containing DPPE-PEG5000, or 200 nm for the formulation without DPPE-PEG5000.

Elaboration of anionic PLGA particles by emulsification-solvent evaporation

An aqueous solution of PVA (0.5% w/v) was prepared by dissolving 150 mg of PVA in 30 mL of Milli-Q water. In order to prepare an aqueous suspension of particles (15 $mg.mL^{-1}$), 60 mg of PLGA were solubilized in 1.5 mL of DCM in a glass vial under magnetic stirring. Then, 4 mL of the PVA solution were added in the vial, followed by vortexing for 20 s to form a coarse emulsion. A fine emulsion was obtained by sonication for 90 s (20% of power),

using a sonicator probe (Sonopuls HD 2070, BANDELIN Electronic GmbH & Co, Berlin, Germany). The size of the oil droplets was further reduced by a second sonication step, in an ice bath (30 s, 10% of power). The solvent (DCM) was evaporated overnight under a gentle magnetic stirring. For confocal microscopy observations, fluorescent PLGA particles were prepared by following the same method, and by adding 0.2 mg of PLA-rhodamine B in the PLGA DCM solution, as previously described[56, 57].

Elaboration of LipoParticles from cationic liposomes and anionic PLGA particles

The elaboration of LipoParticles was previously achieved, and described[18, 19, 20, 21, 22, 23, 24, 25, 27, 28, 29]. Briefly, LipoParticles were prepared by adding an excess of the preformed cationic liposomes to a dispersion of anionic PLGA particles in water. This excess is defined by surface area considerations, expressed by the specific Av/Ap ratio (where Av is the total surface area of liposomes, and Ap is the total surface area provided by polymer particles, as previously detailed[21]), which was equal to 5 for all experiments described in this paper. The mixture was stirred at 650 rpm for 1 h at 70°C. Under such conditions, the adsorption and spreading of cationic liposomes upon contact with the anionic PLGA particles lead to a lipid coating formation onto the particle surface.

Characterization of cationic liposomes, PLGA particles, or LipoParticles by dynamic light scattering (DLS)

Mean hydrodynamic diameters (*Dz*) and mean size distributions (PDI) were determined at 25°C in deionized water by dynamic light scattering (DLS, Zetasizer NanoZS, Malvern Instrument, U.K.). The PDI value is a dimensionless measurement of the size distribution broadness. The measurement angle was 173°, the laser was a helium-neon type operating at

633 nm, and the solvent refractive index and viscosity at 25°C were 1.33 and 0.8904 cP, respectively. For all the samples analyzed, their dilution in water was *ca* 20. Typically, three independent measurements were recorded to obtain average size and size distribution.

215

Characterization of cationic liposomes, PLGA particles, or LipoParticles by electrophoretic mobility measurements (zeta potential measurements)

The electrophoretic mobility values were measured at 25°C in deionized water using a Zetasizer NanoZS apparatus (Malvern Instrument, U.K.). Electrophoretic mobility (μ_e) was 220 converted to zeta potential (ζ) value according to the following Smoluchowski's equation.

$$\mu_e = \frac{\varepsilon_0 . \varepsilon_r}{\eta} \zeta$$

where η, ε_o and ε_r are the medium viscosity, permittivity of vacuum, and relative permittivity, respectively. As for the DLS analyses, the dilution in water of all the samples analyzed was *ca* 20, and three independent measurements were recorded to obtain a mean ζ value.

225

Characterization of cationic liposomes, PLGA particles, or LipoParticles by transmission electron microscopy (TEM)

For transmission electron microscopy (TEM) experiments, a drop (*ca* 5µL) of 0.5% (w/v) particle dispersion was disposed onto a 200 mesh copper grid coated with a carbon film 230 (EMS), and stained with sodium silico tungstate (1% w/v in water) purchased from Sigma Chemical Co. (St. Louis, MO, USA). Then, the grids were transferred into the vacuum column of TEM microscope (PHILIPS CM120, CTµ Lyon, camera Gatan Orius200 2Kx2K). The accelerating voltage used for the observations was 120 kV.

235 **Characterization of LipoParticles by cryo-TEM**

The high resolution 200kV FEI Tecnai F20 is designed to produce optimum high resolution performance in TEM. Cryo-TEM images of LipoParticles (with a DPPC/DPTAP 10/90 molar

ratio coating) were acquired on this microscope equipped with a field emission gun of 200 keV, and a 4kx4k Eagle FEI camera.

240

Study of freeze-drying and re-hydration in water of PLGA particles or LipoParticles

The freeze-drying treatment was carried out thanks to a Freezone 6 Plus® freeze-drier from Labconco, Kansas City, MO, USA. Firstly, the samples (PLGA particles, LipoParticles, without or with trehalose at a final concentration of 10 $mg.mL^{-1}$) were immersed in liquid 245 nitrogen, then placed in the freeze-drier. The pressure was lowered to get a high vacuum, at a temperature of - 83°C for 48 h. Finally, the obtained lyophilisates were re-hydrated with water.

Study of cytotoxicity of cationic liposomes, PLGA particles, or LipoParticles

250 The human osteoblast cell line MG63 (CRL-1427, LGC Standards, USA) was routinely cultured in a complete cell culture medium (DMEM supplemented with 10% of fetal bovine serum 100 $U.mL^{-1}$ penicillin, and 100 $mg.L^{-1}$ streptomycin, from Gibco™, Paisley, UK) in a humidified incubator at 37°C in a 5% CO_2 atmosphere. The goal of the addition of FCS is to provide attachment factors, nutrients, and hormones for mammalian cells. For cytotoxicity 255 evaluations, cells were seeded in 96-well plates at a density of 25,000 cells per well, then they were exposed for 24 h at 37°C to different colloids studied in this work (liposomes, PLGA particles, and LipoParticles), as well as amino-polystyrene particles (used as a positive control). Unexposed cells were used as negative control. The lipid formulations of liposomes and LipoParticles were DPPC/DPTAP 10/90 or DPPC/DPTAP/DPPE-PEG5000 8/90/2 molar 260 ratio with an initial concentration of 7.6 $mg.mL^{-1}$ in bidistillated water. Liposomes, as well as PLGA particles, were incubated with MG63 osteoblasts at increasing concentrations, from 19.5 to 1,250 $\mu g.mL^{-1}$. Finally, LipoParticles (prepared with PLGA particles with a final solid

content of 0.2%, a final liposome concentration of 0.7 mM, Av/Ap of 5) were incubated with MG63 osteoblasts at same different lipid concentrations. For the positive control, amino-polystyrene particles were incubated for 24 h at a concentration of 100 µg.mL^{-1}. 5 replicates were performed per condition to ensure statistical robustness, and this experimental series was carried out 3 times (leading to an analysis number of 15 for each point). After incubation of MG63 cells, their metabolic activity was quantified using the WST-1 assay, following the manufacturer's instructions. This assay is based on the cleavage of the WST-1 tetrazolium salt by dehydrogenases from viable cells to form formazan, which shows an absorbance at 440 nm. Briefly, after the cell incubation, the exposure medium was replaced by 100 µL of a 1/10 (vol./vol.) WST-1 solution, then incubated at 37°C for 1 h. Cell viability was deduced from the comparison of absorbance at 440 nm in the wells of exposed cells to that of wells of unexposed cells.

Characterization of osteoblast internalization of cationic liposomes, PLGA particles, or LipoParticles by confocal laser scanning microscope (CLSM)

Microscope coverslips (thickness 0.13-0.16 mm, Karl Hecht™) were deposited in a culture plate, in which human osteoblast cell line MG63 (CRL-1427, LGC Standards, USA) were cultured in a complete cell culture medium (Dulbecco's Modified Eagle Medium, DMEM, Gibco™, supplemented with 10% FCS, Gibco™) for 24 h without stirring at 37°C under 5% of CO_2. When the number of cells by well was *ca* 40,000, the cultures were washed 2 times with 1 mL of PBS, then different colloids (liposomes, PLGA particles, or LipoParticles) were added to get a final number of colloids per osteoblast of 3,000. Osteoblasts were incubated for 24 h at 37°C under 5% of CO_2 without stirring. Then, the cell culture medium was eliminated, and the cultures were washed 2 times with 1 mL of PBS in order to eliminate colloids which were not internalized in osteoblasts. With the aim of fixing osteoblasts on the microscope

coverslips, these cells were incubated for 30 min at 20°C with 1 mL of formaldehyde (at 4% vol./vol. in PBS). The cultures were washed 3 times with 1 mL of PBS. The staining of osteoblasts was realized in 3 steps. Firstly, the osteoblasts were permeabilized by incubating them for 10 min in ice with a solution of Triton™ X-100 at 0.1% in PBS. Then, the cultures were washed 3 times with PBS before being incubated with a BSA solution at 10 $mg.mL^{-1}$ for 30 min at 25°C, then washed 3 times with 1 mL of PBS. Finally, the actin was stained by adding 200 µL of a Alexa Fluor 647 phalloidin (Invitrogen ThermoFisher) solution at 165 nM in PBS in each well. The osteoblasts were kept for 20 min at 20°C in the dark before washing them 5 times with 1 mL of PBS. Osteoblasts were fixed by incubating them for 30 min in the dark at 20°C with 1 mL of formaldehyde (4% vol./vol. in PBS). The cultures were washed 3 times with PBS, and then with sterile water Versol®. The microscope coverslips on which the osteoblasts were developed were hermetically closed (with a nail polish) on a microscopy slide, and the excess of sample was eliminated with Kimwipes® paper. Finally, this final microscope slide was observed thanks to a confocal laser scanning microscope (CLSM LSM 800 Zeiss, Jena, Germany) under a 40x or 63x oil immersion objectives. The images were acquired with a Zen23® software and were analyzed with Image J®.

Concerning different staining agents used, MG63 osteoblast cells have been stained by using the Alexa Fluor 647 phalloidin (which reveals the actin filaments, excitation/emission wavelengths = 650/668 nm). The PLGA particles were stained with rhodamine B (excitation/emission wavelengths of rhodamine B = 530/590 nm), and finally, lipid membranes were stained by incorporating a TopFluor®-PC fluorescent lipid in lipid formulation at 1% molar ratio (excitation/emission wavelengths of TopFluor®-PC = 495/503 nm). Note that it was previously checked that the fluorescence of each staining agent (*i.e.*, Alexa Fluor 647 phalloidin, TopFluor®-PC lipid, and rhodamine B) was specific of

fluorescence filter used to observe each of them, and there was no fluorescence "bleed-through" between them.

Characterization of osteoblast internalization of cationic liposomes, PLGA particles, or LipoParticles by flow cytometry

The human MG63 cells were seeded (*ca* 50,000 cells per well) in 24 well plate (Falcon, Le Pont de Claix, France) in a complete cell culture medium in a humidified incubator for 48 h at 37°C in a 5% CO_2 atmosphere. When the number of osteoblasts per well was 100,000, cultures were washed 2 times with PBS, then different colloids (liposomes, PLGA particles, or LipoParticles) were added with a colloid number of 22,000 per osteoblast for 24 h. One step of rinsing was achieved in order to eliminate colloids non internalized in osteoblasts. The wells were washed 2 times with PBS, then osteoblasts were dissociated by trypsinization (0.05% Trypsin-EDTA 1X, Gibco™) in order to put them in suspension in a Falcon® tube. Osteoblasts were stained with LIVE/DEAD™ kit (Invitrogen®). The Falcon® tubes were centrifuged at 1,500 rpm for 5 min, the supernatants were removed, and the pellets were washed with 1 mL of PBS. A new centrifugation step was applied at 1,500 rpm for 5 min, the supernatants were removed, and the pellets were resuspended in PBS. Osteoblasts were incubated with 100 µL of formaldehyde (at 37% vol/vol in PBS) for 30 min at 20°C in the dark. Cells were centrifuged at 1,500 rpm for 5 min, the supernatants were removed, and the pellets were washed with PBS containing BSA at 1% wt. A second centrifugation step (for 5 min at 1,500 rpm) was applied in order to eliminate PBS. The pellets were resuspended in PBS containing BSA at 1% wt in order to get $1x10^6$ osteoblasts per mL. The samples were analyzed with FACS LSR II 4 lasers cytometer (TopFluor®-PC and rhodamine B were excited at 488 nm and 561 nm, and their emission were measured at 525/50 nm and 582/15

nm, respectively). The events (*ca* 20,000) were among the « individual live cells » events. The data were acquired and analyzed with BD FACSDiva® software.

Observations of MG63 cells infected by intracellular *Staphylococcus aureus* in presence or not of PLGA particles, or LipoParticles, by TEM on ultrathin sections

Internalization of PLGA particles and LipoParticles inside MG63 osteoblastic cells infected by *Staphylococcus aureus* was assessed by TEM on ultrathin sections. MG63 cells were seeded at 350,000 osteoblasts per well into 6-well tissue culture plates (Falcon, Le Pont de Claix, France), and cultured for 48 h until 70%-80% confluence. *Staphylococcus aureus* HG001 was used to carry out the intracellular infection. The day of the infection, the number of osteoblasts in each well was evaluated to adjust the bacterial suspension at a multiplicity of infection (MOI) of 10 bacteria per cell. Then the adjusted bacterial suspension was added to the osteoblastic cell culture wells for 2 h to allow the bacterial internalization. Cells were then washed twice with PBS and were treated with culture medium containing 10 µg/mL of lysostaphin (Sigma-Aldrich, Saint-Louis, MO, US) to kill all remaining extracellular bacteria without affecting intracellular bacteria. After 1 h of lysostaphin treatment, cells were washed twice with PBS, and PLGA particles or LipoParticles suspensions were added to the infected cells at 22,000 colloids/osteoblast. A control with non-treated infected osteoblasts was also performed. After 24 h, osteoblasts were washed with PBS, fixed with a solution containing 1 volume of cell culture medium, and 1 volume of glutaraldehyde 4% for 15 min at 4°C, and the solution was replaced with another containing 1 volume of glutaraldehyde 4% and 1 volume of cacodylate 0.2 M pH 7.4. After washing three times with a 0.2 M sodium cacodylate buffer, cells were post-fixed with 1% w/v aqueous osmium tetroxide at room temperature for 1 h, and dehydrated in a graded series of ethanol at room temperature, and embedded in an Epon resin. After polymerization, ultrathin sections (100 nm) were cut with a

UC7 (Leica) ultramicrotome, and collected on formvar/carbon-coated 200 hexagonal mesh copper grids. Sections were stained with uranyl acetate and lead citrate before their observation on a Jeol 1400JEM (Tokyo, Japan) TEM equipped with a Orius 1000 camera and Digital Micrograph.

365

Results and Discussion

Before studying the internalization of LipoParticles in a human osteoblast cell line (MG63) by confocal laser scanning microscopy, flow cytometry assays, and TEM on ultrathin sections, LipoParticles have been elaborated according to a contact/fusion process of cationic
370 liposomes onto the anionic surface of PLGA particles. Then, the resulting assemblies were thoroughly characterized by DLS, zetametry, and (cryo)TEM. Their colloidal stability following a dilution in PBS or in a cell culture medium, their freeze-drying/re-hydration in water, as well as their cytotoxicity towards the same osteoblast cell line (MG63) have also been investigated.

375

Elaboration and characterization of LipoParticles obtained from an assembly of cationic liposomes and anionic PLGA particles

As previously mentioned, the elaboration of LipoParticles occurs thanks to a contact/fusion process of many liposomes onto the surface of polymer particles. Thus, the reorganization of
380 lipid membranes from liposomes onto the particle surface leads to core-shell LipoParticles, that is to say polymer particles coated with lipid membranes. To this end, liposomes and polymer particles were independently prepared before mixing of both (at 650 rpm for 1 h at 70°C). Our choice of polymer for the particles was PLGA for all the reasons (FDA approved, biocompatibility, and biodegradability) cited in the introductive part. PLGA particles were
385 synthesized by an oil-in-water emulsion method using PVA as a surfactant. Their zeta

potential (ζ) is slightly anionic (- 4.5 mV, Table 1) due to carboxylic acid end-groups of PLGA chains. As shown by TEM (Figure 1A), these particles are spherical, with a number-average diameter (*Dn*) of *ca* 80 nm (calculated on 315 particles by Image J®, see other images in SI1). The average hydrodynamic diameter (*Dz*) measured by DLS was found to be much higher (303 ± 44 nm, Table 1), with a relatively narrow size distribution (PDI < 0.2, Table 1). The significant size difference revealed by both analysis techniques could be explained by the type of size average. Indeed, an average in intensity of particle sizes was obtained with a DLS analysis. An average in intensity is much more impacted by the biggest particles in a mixture than an average in number calculated from TEM images. To illustrate this difference between an average in intensity and an average in number, the following example of calculation can be carried out. A mixture of 1% (in number) of 300 nm particles with 99% (in number) of 80 nm ones leads for this mixture to a diameter average in intensity of 299.99 nm, and an average in number of 82.20 nm.

Concerning the liposomes, they were elaborated by the Bangham method followed by an extrusion step through a polycarbonate membrane of porosity equal to 100 nm or 200 nm for the lipid formulations with or without DPPE-PEG5000, respectively. Indeed, two liposomal formulations were elaborated in this work for comparison: DPPC/DPTAP 10/90 molar ratio, and DPPC/DPTAP/DPPE-PEG5000 8/90/2 molar ratio (DPPC is a zwitterionic lipid, DPTAP, a cationic one, and DPPE-PEG5000, a lipid bearing on its polar head a PEG chain of 5,000 $g.mol^{-1}$). Both lipid formulations correspond to cationic liposomes (due to 90% mol. of cationic DPTAP lipids) in order to improve their contact and their fusion onto the anionic particle surface *via* electrostatic attractions. The goal of the final extrusion step is to drastically decrease the size distribution of liposomes. As a result, the PDI value of the elaborated liposomes is very low since below 0.1 (Table 1). About their sizes measured by DLS, they are around 110-130 nm (Table 1), and their morphology is spherical according to the TEM

analysis (Figure 1B). As expected, their sign of zeta potential (ζ) is positive due to the presence of cationic DPTAP lipids in the formulation (Table 1). Finally, note that the presence of lipid-PEG conjugates at 2% molar ratio in the lipid formulation does not have any influence on *Dn*, *Dz*, PDI, and zeta potential values (Table 1).

Table 1. Number-average diameters (*Dn*) measured by TEM, average hydrodynamic diameters (*Dz*), size distributions (PDI) measured by DLS, and zeta potentials (ζ) measured by zetametry of PLGA particles, liposomes (DPPC/DPTAP 10/90 molar ratio or DPPC/DPTAP/DPPE-PEG5000 8/90/2 molar ratio), and resulting LipoParticles obtained by spontaneous adsorption of lipid membranes onto PLGA particles. Measurements were performed after a 20-fold dilution in deionized water.

	Dn (nm) TEM	*Dz* (nm) DLS	PDI DLS	ζ (mV)
Liposomes DPPC/DPTAP 10/90 molar ratio	158 ± 33 N_o = 500	136 ± 11 N_b = 16	0.08 ± 0.02 N_b = 16	+ 44 ± 4 N_b = 16
Liposomes DPPC/DPTAP/DPPE-PEG5000 8/90/2 molar ratio	ND	111 ± 12 N_b = 10	0.09 ± 0.04 N_b = 10	+ 44 ± 6 N_b = 10
PLGA particles	79 ± 39 N_o = 315	303 ± 44 N_b = 26	0.17 ± 0.04 N_b = 26	- 4.5 ± 4.8 N_b = 25
LipoParticles DPPC/DPTAP 10/90 molar ratio	ND	271 ± 40 N_b = 6	0.18 ± 0.02 N_b = 6	+ 8.0 ± 2 N_b = 6
LipoParticles DPPC/DPTAP/DPPE-PEG5000 8/90/2 molar ratio	ND	260 ± 33 N_b = 6	0.19 ± 0.02 N_b = 6	+ 4.0 ± 1 N_b = 6

With N_o = number of considered objects for the calculations of averages by using Image J®, N_b = number of different batches used. ND = not determined.

As mentioned before, the driving force of the reorganization of liposomes onto the polymer particle surface is of electrostatic nature between cationic liposomes and anionic particles, with opposite surface charges. Moreover, in order to facilitate this reorganization, a surface area excess of liposomes in comparison of particle one was used (Av/Ap = 5, see the explanations in experimental section). The observation of an inversion of zeta potential sign of final assemblies (LipoParticles) *versus* the polymer particle one (*ca* + 4 or + 8 mV for final LipoParticles *versus* - 4.5 mV for PLGA particles) confirms a surface modification of PLGA particles by cationic lipids. The average size of LipoParticles is around 265 nm with a PDI below 0.2 demonstrating that this lipid reorganization process does not lead to aggregated assemblies. Note that the size of resulting LipoParticles is slightly below the one of initial PLGA particles (*ca* 300 nm). This could be explained by the fact that the DLS measurement takes also into account the excess of liposomes (with a lower size than particle one, 110 - 130 nm) in the determination of the average size.

The lipid membrane coating of particles is usually tricky to observe on TEM images because its thickness is much lower than the particle size (*i.e.*, a thickness of *ca* 5 nm in comparison with 300 nm for the particle size). Nevertheless, it can be distinguished on TEM images of Figure 1C (as highlighted by the red arrows, more images are presented in SI1 showing also this lipid coating).

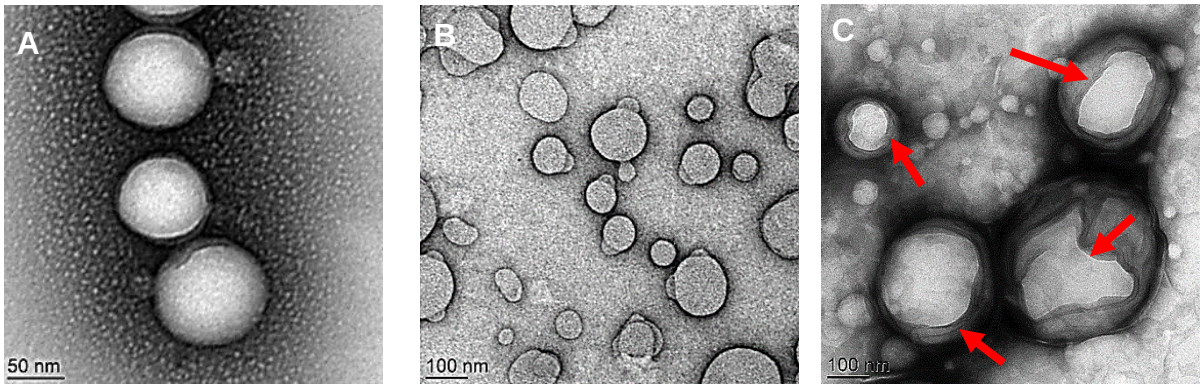

Figure 1. TEM images of PLGA particles (A), DPPC/DPTAP 10/90 molar ratio cationic liposomes (B), LipoParticles (Av/Ap = 5) with a PLGA core and a DPPC/DPTAP 10/90 molar ratio coating (C). Red arrows highlight the lipid coating onto the PLGA particles. All samples were stained with sodium silico tungstate at 1% w/v in water. More images of PLGA particles, and LipoParticles are presented in SI1.

This lipid membrane coating of the PLGA particle surface was also confirmed by cryo-TEM, and by using a high resolution Tecnai F20 microscope. Indeed, cryo-TEM images of a fast-frozen suspension of LipoParticles display a more or less continuous fringe (indicated by red arrows in Figure 2) at a distance estimated to 4 nm around the particles. This distance corresponds to the separation between two electron-dense layers in a liposome, demonstrating that the particles are well covered with a lipid bilayer.

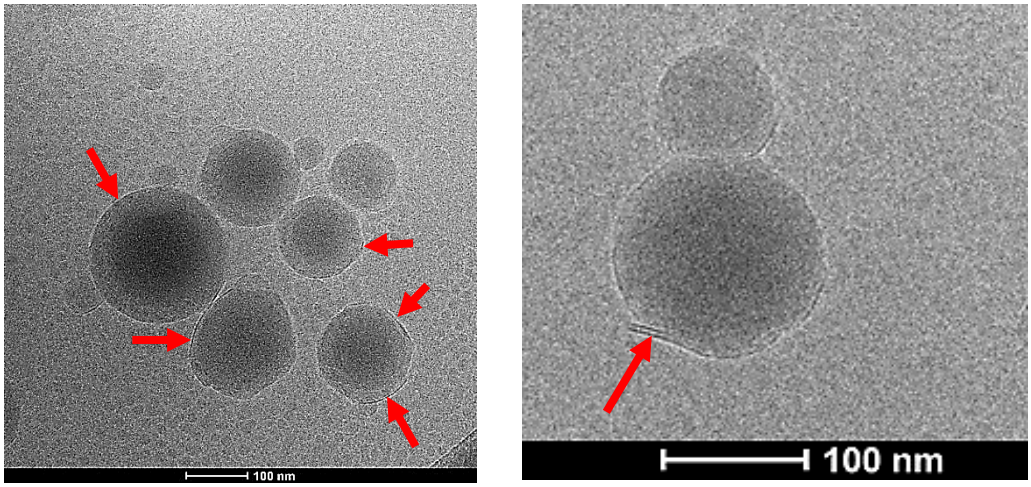

Figure 2. Cryo-TEM images of LipoParticles constituted of a PLGA core and a DPPC/DPTAP 10/90 molar ratio coating acquired on a high resolution Tecnai F20 microscope equipped with a field emission gun of 200 keV, and a 4kx4k Eagle FEI camera.

Study of the colloidal stability of the LipoParticles after their dilution in PBS or in a cell culture medium

In order to carry out a study of interactions between cells and LipoParticles, it was necessary to previously examine that the PLGA particles and the LipoParticles do not form aggregates in PBS 1X (pH 7.4), nor in the Dulbecco's modified eagle medium (DMEM, supplemented with 10% FCS) cell culture medium (CCM) used for *in vitro* investigations. To this end, LipoParticles were prepared in water and 20-fold diluted in each one of these media, and characterized by DLS (Table 2). In water, the DLS average size of PLGA particles was found to be *Dz* = 303 ± 44 nm with a PDI value of 0.17 (Table 1). Consequently, their dispersion in PBS 1X and CCM did not lead to changes (*Dz* = 309 ± 5 nm, PDI = 0.19 ± 0.01, and *Dz* = 326 ± 13 nm, PDI = 0.23 ± 0.02, respectively). Concerning the LipoParticles with a DPPC/DPTAP 10/90 molar ratio formulation, in water, their size was found to be 271 ± 40 nm (PDI = 0.18 ±0.02, Table 1). After their dispersion in PBS 1X and CCM, a significant increase of their size was detected (514 ± 84 nm and 566 ± 53 nm, respectively, Table 2), revealing the formation of aggregates, and their colloidal instability in these media. However, when 2% mol. of DPPE-PEG5000 conjugates were added in their lipid formulation, the dispersion of LipoParticles in PBS 1X and CCM did not cause a size change (272 ± 2 nm, and 307 ± 4 nm, respectively, Table 2, instead of 260 ± 33 nm in water, Table 1). In conclusion, this lipid formulation containing lipid-PEG5000 conjugates at 2% mol. allows to satisfactorily ensure the colloidal stability of LipoParticles in PBS 1X and CCM.

Table 2. Average hydrodynamic diameters (*Dz*), size distributions (PDI) measured by DLS of PLGA particles, and LipoParticles (DPPC/DPTAP 10/90 molar ratio or DPPC/DPTAP/DPPE-PEG5000 8/90/2 molar ratio) after their 20-fold dilution in PBS 1X or cell culture medium (CCM). N_b = number of different batches used = 6.

	PBS 1X		CCM	
	Dz (nm)	PDI	*Dz* (nm)	PDI

PLGA particles	309 ± 5	0.19 ± 0.01	326 ± 13	0.23 ± 0.02
LipoParticles DPPC/DPTAP 10/90 molar ratio	514 ± 84	0.16 ± 0.02	566 ± 53	0.26 ± 0.01
LipoParticles DPPC/DPTAP/DPPE-PEG5000 8/90/2 molar ratio	272 ± 2	0.20 ± 0.02	307 ± 4	0.24 ± 0.01

Study of the freeze-drying and re-hydration in water of PLGA particles or LipoParticles

Freeze-drying is a process frequently used in industry to facilitate the storage and the shipping of some pharmaceutical products which are thermolabile or which show instabilities in aqueous solution during several months of storage. At the same time, this freeze-drying process allows the sterilization of pharmaceutical compounds. In this context, the possibility to perform a freeze-drying of LipoParticles after their elaboration was examined.

For the sake of comparison, same freeze-drying conditions were also applied to PLGA particles (with an initial solid content of 1.6% w/w). A dilution of 8-fold in water of PLGA particles (final solid content = 0.2% w/w), and a freeze-drying during 48 h were employed. The obtained lyophilisates were re-hydrated, and analyzed by DLS. Table 3 shows that freeze-drying of PLGA particles causes their aggregation as suggested by the increase in average hydrodynamic size and PDI value of 20% and 32%, respectively.

The same study was achieved on LipoParticles with the two previous lipid formulations (DPPC/DPTAP 10/90 molar ratio, and DPPC/DPTAP/DPPE-PEG5000 8/90/2 molar ratio). In this case, Table 3 displays that the freeze-drying of LipoParticles without DPPE-PEG5000 (*i.e.*, with a DPPC/DPTAP 10/90 molar ratio) leads also to an increased size and PDI value of 16% and 34%, respectively, demonstrating that this lipid formulation is not suited to be freeze-dried. At the opposite, as for the study of the colloidal stability of LipoParticles in PBS 1X and CCM, the presence of 2% mol. of lipid-PEG5000 conjugates in the lipid formulation

allows them to be stabilized during the freeze-drying/re-hydration process. Indeed, relatively low variations in size and PDI value (7% and 13%, respectively) were observed (Table 3). This suggests that this type of LipoParticles do not aggregate during the freeze-drying process, likely due to the steric stabilization provided by the presence of PEG chains onto the surface of these LipoParticles.

Table 3. Average hydrodynamic diameters (*Dz*), size distributions (PDI) measured by DLS of PLGA particles, LipoParticles (DPPC/DPTAP 10/90 molar ratio or DPPC/DPTAP/DPPE-PEG5000 8/90/2 molar ratio) before or after freeze-drying/re-hydration without or with trehalose (at 10 $mg.mL^{-1}$).

	***Dz* (nm)**	**PDI**
PLGA particles		
Before freeze-drying	430 ± 7	0.19 ± 0.03
After freeze-drying	536 ± 11	0.28 ± 0.01
Difference (%)	**+20**	**+32**
LipoParticles DPPC/DPTAP 10/90		
Before freeze-drying	379 ± 4	0.19 ± 0.01
After freeze-drying	449 ± 30	0.29 ± 0.03
Difference (%)	**+16**	**+34**
LipoParticles DPPC/DPTAP/DPPE-PEG5000 8/90/2		
Before freeze-drying	329 ± 3	0.20 ± 0.01
After freeze-drying	354 ± 5	0.23 ± 0.01
Difference (%)	**+7**	**+13**
PLGA particles with Trehalose		
Before freeze-drying	439 ± 1	0.16 ± 0.04
After freeze-drying	471 ± 6	0.12 ± 0.02

Difference (%)	**+7**	**-33**
LipoParticles DPPC/DPTAP 10/90 with Trehalose		
Before freeze-drying	333 ± 10	0.18 ± 0.03
After freeze-drying	326 ± 9	0.21 ± 0.02
Difference (%)	**-2**	**+14**
LipoParticles DPPC/DPTAP/DPPE-PEG5000 8/90/2 with Trehalose		
Before freeze-drying	327 ± 4	0.18 ± 0.03
After freeze-drying	330 ± 5	0.22 ± 0.01
Difference (%)	**+1**	**+18**

According to Abdelwahed *et al.*[58], Shulkin *et al.*[59], Stark *et al.*[60], Van den Hoven *et al.*[61], Chaudhury *et al.*[62], freeze-drying is a process that requires the presence of a cryoprotectant agent in the sample to prevent it of aggregation phenomena. For this purpose, the most used chemical compounds used in literature are sugars, notably the trehalose molecule which has the property to be localized at the interface of colloids in suspension, and to decrease their glass transition temperature. This provides some "flexibility" to colloids during the freezing step which protects them of mechanical stress and aggregation provoked by the formation of glass crystals. In this context, with the aim of circumventing such an aggregation of PLGA particles and LipoParticles without lipid-PEG conjugates, trehalose agent was added to formulations. Vega *et al.*[63] have used it at a final concentration of 10 $mg.mL^{-1}$ in water to carry out a freeze-drying of PLGA particles without leading to their aggregation. The samples of PLGA particles and LipoParticles (final solid content of 0.2% w/w) were consequently prepared in our work with such a trehalose concentration, and a 48 h duration of freeze-drying.

In these conditions, the size and PDI value evolutions of PLGA particles (Table 3) displays that the freeze-drying process in the presence of trehalose leads to a low increase of 7% in size

(and a decrease of -33% in PDI value). This seems to prove that the freeze-drying process does not imply aggregation of particles thanks to trehalose cryoprotectant agent.

The same study was performed on LipoParticles with DPPC/DPTAP 10/90 molar ratio or DPPC/DPTAP/DPPE-PEG5000 8/90/2 molar ratio (final solid content of 0.2% w/w). They were freeze-dried during 48 h, with a final trehalose concentration of 10 $mg.mL^{-1}$. Concerning LipoParticles with DPPC/DPTAP 10/90 molar ratio, the presence of trehalose prevents them of an aggregation (modifications of only 2% in size, and 14% in PDI value). For LipoParticles with DPPC/DPTAP/DPPE-PEG5000 8/90/2 molar ratio, the average size has only increased of 1% in size and 18% in PDI value. Note that in this case, the results in the presence of trehalose are similar to those obtained in its absence. Indeed, the presence of lipid-PEG5000 conjugates at 2% molar ratio in the lipid membrane of LipoParticles can avoid the trehalose requirement.

Study of the cytotoxicity of liposomes, PLGA particles, and LipoParticles towards MG63 osteoblasts

A cytotoxicity study of PLGA particles, liposomes, and LipoParticles (both with a formulation of DPPC/DPTAP 10/90 molar ratio or DPPC/DPTAP/DPPE DPPE-PEG5000 8/90/2 molar ratio) was performed by exposing for 24 h at 37°C the human MG63 osteoblast cell line to these different samples. Increasing concentrations of these samples from 19.5 to 1,250 $\mu g.mL^{-1}$ were used, and the WST-1 assay was applied (Figure 3). PS-amine particles were used as positive control, and unexposed cells, as a negative control.

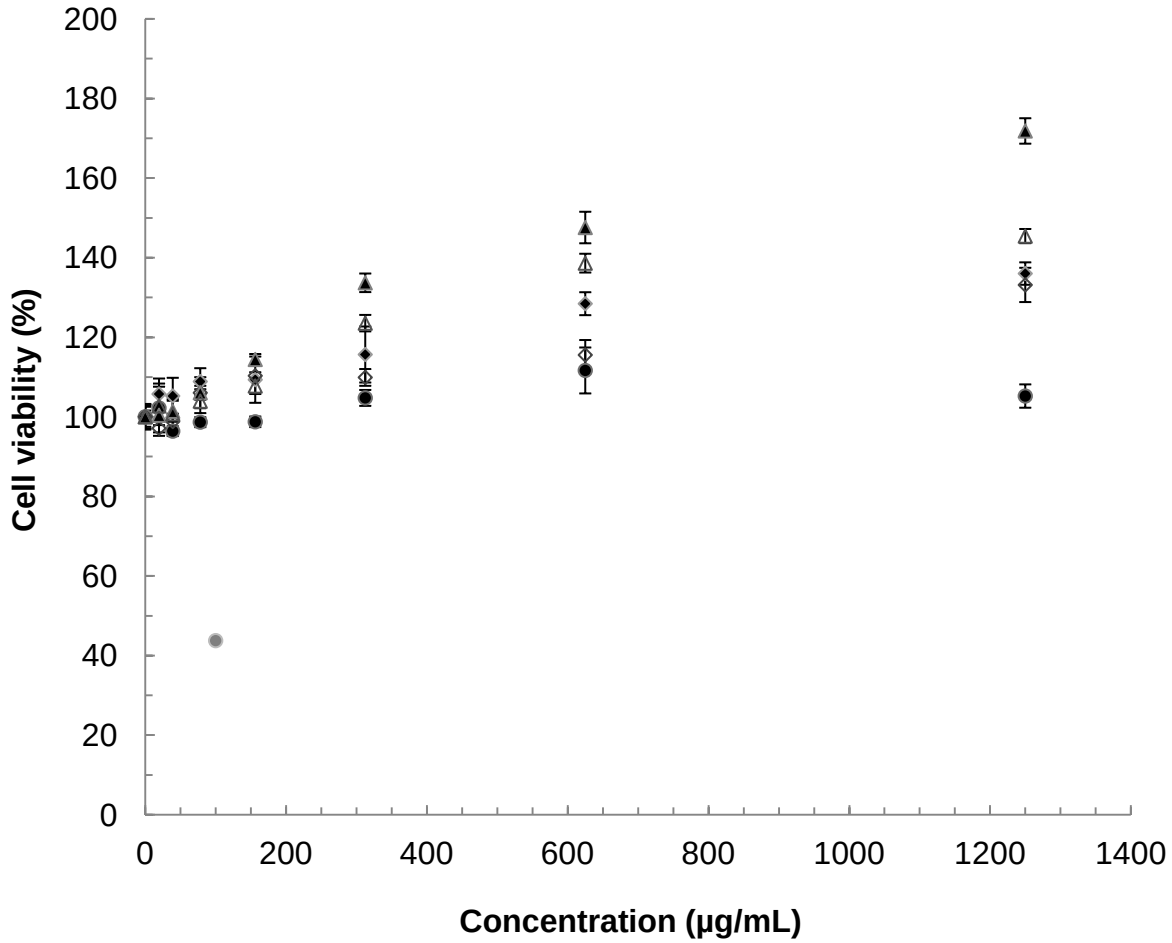

Figure 3. Cytotoxicity assays on MG63 osteoblasts of DPPC/DPTAP 10/90 molar ratio liposomes (Δ), DPPC/DPTAP/DPPE-PEG5000 8/90/2 molar ratio liposomes (▲), DPPC/DPTAP 10/90 molar ratio LipoParticles (◊), DPPC/DPTAP/DPPE-PEG5000 8/90/2 molar ratio LipoParticles (♦), and PLGA particles (●). PS-amine particles, used at 100 µg.mL^{-1} as positive control (●). All the standard deviations were calculated on 15 analyses.

As shown in Figure 3, none of the studied samples has shown any cytotoxicity towards MG63 osteoblasts (excepted, as expected, for the positive control), and even increases in the metabolic activity (> 100%) can be observed for liposomes and LipoParticles (contrarily to PLGA particles), probably due to the cell stimulation by their lipid membranes. All together, these results suggest in a positive way that all our samples can be used for the subsequent phase of our study, in order to examine their interactions with the MG63 osteoblast cell line.

Evidence of an enhanced osteoblast cell internalization of LipoParticles by confocal laser scanning microscopy

Osteoblast cells can be potential reservoirs for *Staphylococcus aureus* in bone and joint infections. Our work focuses on the capacity of all the different assemblies (liposomes, PLGA particles, LipoParticles) to be internalized by osteoblasts, with the aim to attain the bacteria internalized in these cells. To this end, all these assemblies were incubated with MG63 osteoblast cells, and observed by confocal laser scanning microscopy. With the aim of localizing each assembly type by this technique, each one of them has been associated to a specific fluorescent probe. The different staining agents (nature, excitation/emission wavelengths) of osteoblasts, PLGA particles, and LipoParticles are further explained in Experimental Section.

With the aim of maximizing the number of individualized cells observed in confocal laser scanning microscopy, the cell confluence has been limited to *ca* 40,000 osteoblasts in each one of wells of the cell culture plate. Then, liposomes, PLGA particles, or LipoParticles were added and incubated for 24 h at 37°C in CCM (DMEM, supplemented with 10% FCS) with an average amount of 3,000 liposomes, PLGA particles, or LipoParticles per osteoblast cell. Then, MG63 osteoblast cells were treated following the protocol described in "Materials and Methods" part, and were observed with an inverted laser scanning confocal microscope.

Figure 4 shows the resulting images of unexposed MG63 osteoblast cells, and exposed ones to liposomes, PLGA particles, or LipoParticles. Images of unexposed MG63 osteoblast cells (Figure 4A) reveal that the staining of their actin protein filaments by Alexa Fluor 647 phalloidin was efficient since it allows the observation of the wholeness of individualized cells or/and at confluence, in adhesion at the surface of microscope coverslip. The images of liposomes (Figure 4B), without (at the top, Figure 4B) or with PEG chains (at the bottom,

Figure 4B) in their lipid formulation, exhibit a green fluorescence spread throughout the whole cell enlightening that the liposomes, whatever their lipid formulation, were internalized in MG63 osteoblast cells. The elucidation of the cellular internalization mechanisms of liposomes has been the subject of studies described in the literature [64, 65, 66, 67]. This green fluorescence seems to be localized in the cell cytoplasm, and not at the level of cell nuclei (which are consequently well-visualized). It is worthy of note that the confocal laser scanning microscopy being not a quantitative technique in the analysis conditions used herein, it would be hazardous to determine a precise influence of the lipid formulation upon the efficiency of the cell internalization. The images of PLGA particles (appearing in orange due to rhodamine B staining in Figure 4C) disclose, contrary to liposomes, a low, even no, internalization of them by MG63 osteoblast cells. These particles are rather homogenously dispersed on the microscope coverslip, likely irreversibly attached to it (since not removable by the washes). The slightly negative PLGA particle surface (ζ = - 4.5 ± 4.8 mV, Table 1), and/or eventual protein corona (coming from CCM) adsorbed onto particles, could explain a difficult internalization of them inside negative-surface cells could explain their difficult internalization inside negative-surface cells. This charge effect on the cell uptake has already been studied[47].

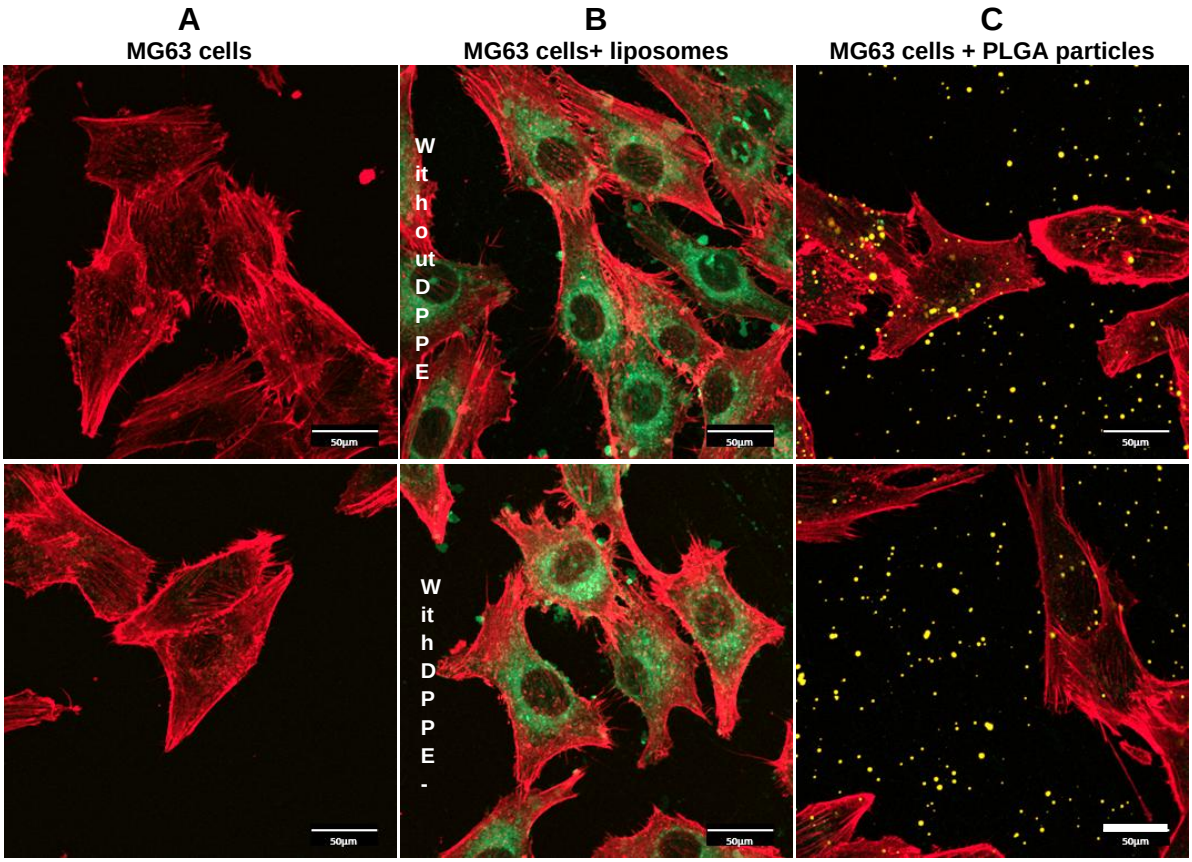

Figure 4. Confocal laser scanning microscopy analysis of MG63 osteoblast cells (A), and *in vitro* uptake in these MG63 osteoblast cells of liposomes composed of DPPC/DPTAP/TopFluor®-PC 9/90/1 molar ratio (top) or DPPC/DPTAP/DPPE-PEG5000/TopFluor®-PC 7/90/2/1 molar ratio (bottom) (B), as well as PLGA particles (C) after an incubation for 24 h at 37°C, under 5% of CO_2, in DMEM supplemented with 10% of FCS with MG63 osteoblast cells. Colors of different staining agents used: red for Alexa Fluor 647 phalloidin (staining the MG63 cells), green for TopFluor®-PC fluorescent lipid (staining the lipid membranes), orange for rhodamine B (staining the PLGA particles). Magnification x40, scale bar = 50 µm.

Finally, concerning the LipoParticles, as for the liposomes, they are localized inside the MG63 osteoblast cells, whatever the lipid formulation used (*i.e.*, without lipid-PEG conjugates in Figure 5, or with lipid-PEG conjugates in Figure 6).

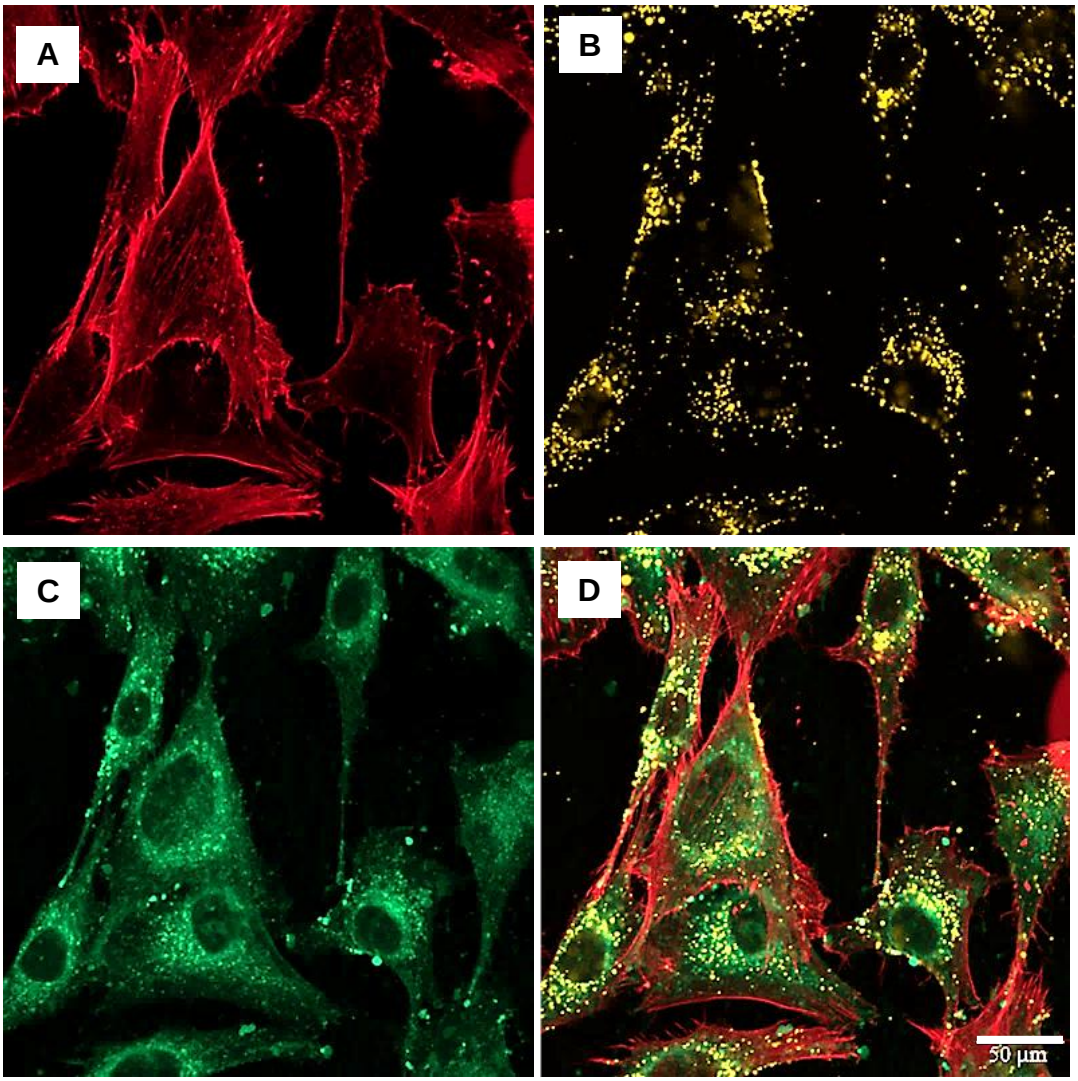

Figure 5. Confocal laser scanning microscopy analysis of *in vitro* uptake of LipoParticles in MG63 osteoblast cells composed of DPPC/DPTAP/TopFluor®-PC 9/90/1 molar ratio and PLGA particles, after their incubation for 24 h at 37°C, under 5% of CO_2, in DMEM supplemented with 10% of FCS with MG63 osteoblast cells. Colors of different staining agents used: A) red for Alexa Fluor 647 phalloidin (staining the MG63 cells), B) orange for rhodamine B (staining the PLGA particles), C) green for TopFluor®-PC fluorescent lipid (staining the lipid membranes), and D) all colors are merged showing the co-localization of different species. Magnification x40, scale bar = 50 µm.

Figures 5D and 6D show an image merging the three staining agents, and three other examples are also provided in SI for each lipid formulation (SI2 for the lipid formulation without lipid-PEG conjugates, and SI3, for one with lipid-PEG conjugates).

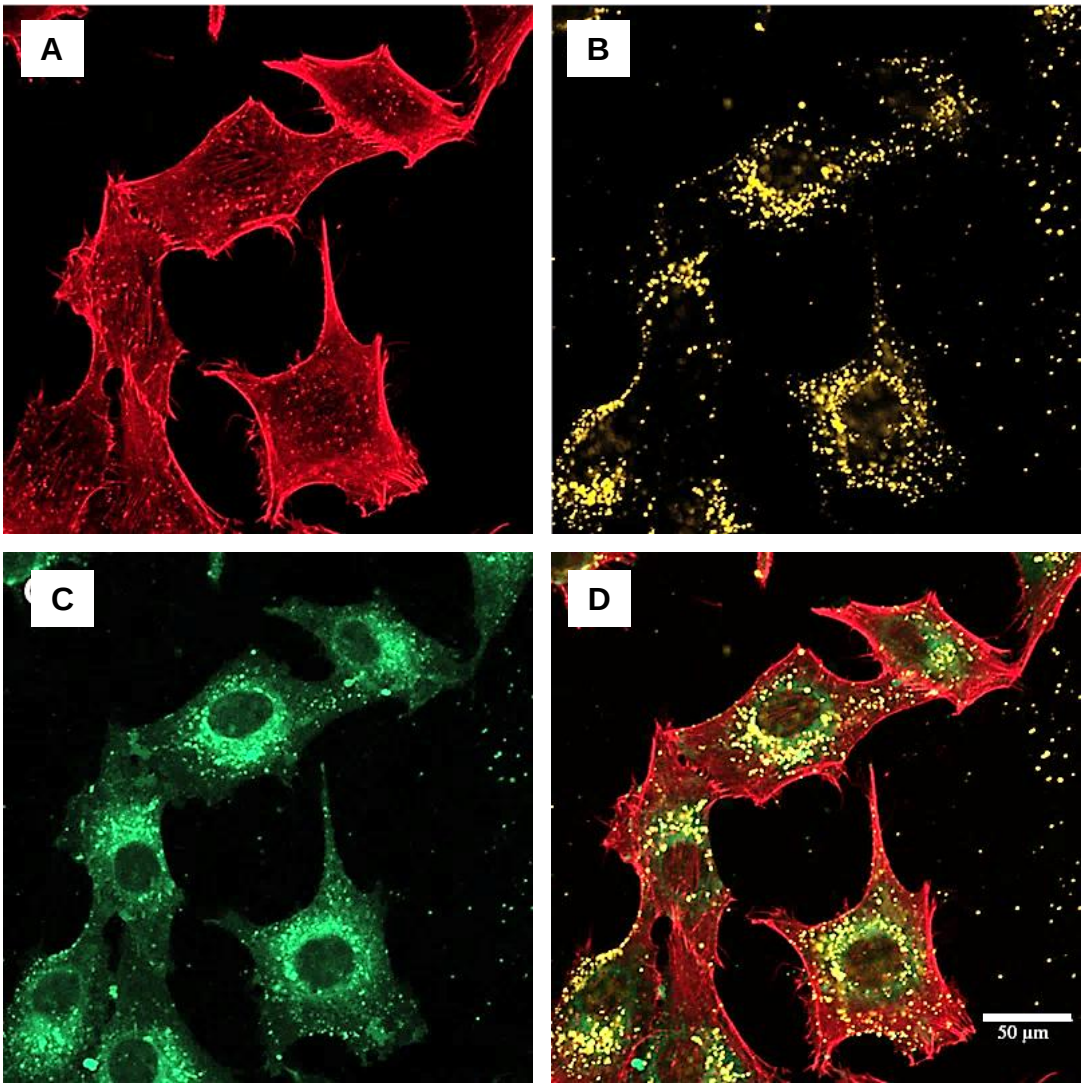

650

Figure 6. Confocal laser scanning microscopy analysis of *in vitro* uptake of LipoParticles in MG63 osteoblast cells composed of DPPC/DPTAP/DPPE-PEG5000/TopFluor®-PC 7/90/2/1 molar ratio and PLGA particles, after their incubation for 24 h at 37°C, under 5% of CO_2, in DMEM supplemented with 10% of FCS with MG63 osteoblast cells. Colors of different
655 staining agents used: A) red for Alexa Fluor 647 phalloidin (staining the MG63 cells), B) orange for rhodamine B (staining the PLGA particles), C) green for TopFluor®-PC

fluorescent lipid (staining the lipid membranes), and D) all colors are merged showing the co-localization of different species. Magnification x40, scale bar = 50 µm.

Figures 5 and 6 highlight the co-localization of staining agents of MG63 osteoblast cells (in red), PLGA particles (in orange) coated with a lipid membrane (in green), that is to say the LipoParticles, whatever the lipid formulation used. Consequently, these images evidence that the lipid coating of PLGA particles allows them to be internalized in MG63 osteoblast cells (since these same PLGA particles, without lipid coating, were not uptaken in the same osteoblast cells, as seen in Figure 4C). Nevertheless, the presence of a few PLGA particles outside osteoblast cells, mainly observed in Figure 5, may suggest an incomplete lipid coating of all the particles despite a liposome excess used (Av/Ap = 5), or/and a partial disorganization of the lipid coating during the incubation (for 24 h at 37°C). Note also that the diffuse green fluorescence detected inside the MG63 osteoblast cells (Figure 5C and Figure 6C) may come from liposomes in excess since we could not purify LipoParticles due to the instability of PLGA particles during the centrifugation step required for such treatment. Finally, for the same reasons as the liposomes, it is not possible to rigorously distinguish a quantitative influence of lipid formulation of LipoParticles (with or without PEG chains) on the cell internalization magnitude by this technique.

With the goal of confirming the internalization of LipoParticles in the MG63 osteoblast cells thanks to their membrane coating, we took advantage of the possibility given by the confocal microscope to make an “optical sectioning”, meaning to acquire a series of subsequent images on the Z axis of the cell (called a “Z-stack”, rendering in this way a 3D imaging). Firstly, this observation mode was used on the microscope coverslip of PLGA particles (without lipid coating) incubated with MG63 osteoblast cells in the same previous

experimental and analysis conditions. Figure 7 shows that these PLGA particles (in orange) are mainly present outside MG63 osteoblast cells (in red), and near the surface of microscope coverslip (Figure 7, a-b), and are absent when the focal plane is situated inside the MG63 osteoblast cell (Figure 7, c-h). This confirms that the PLGA particles, without lipid coating, are a little, or not, internalized inside the MG63 osteoblast cells.

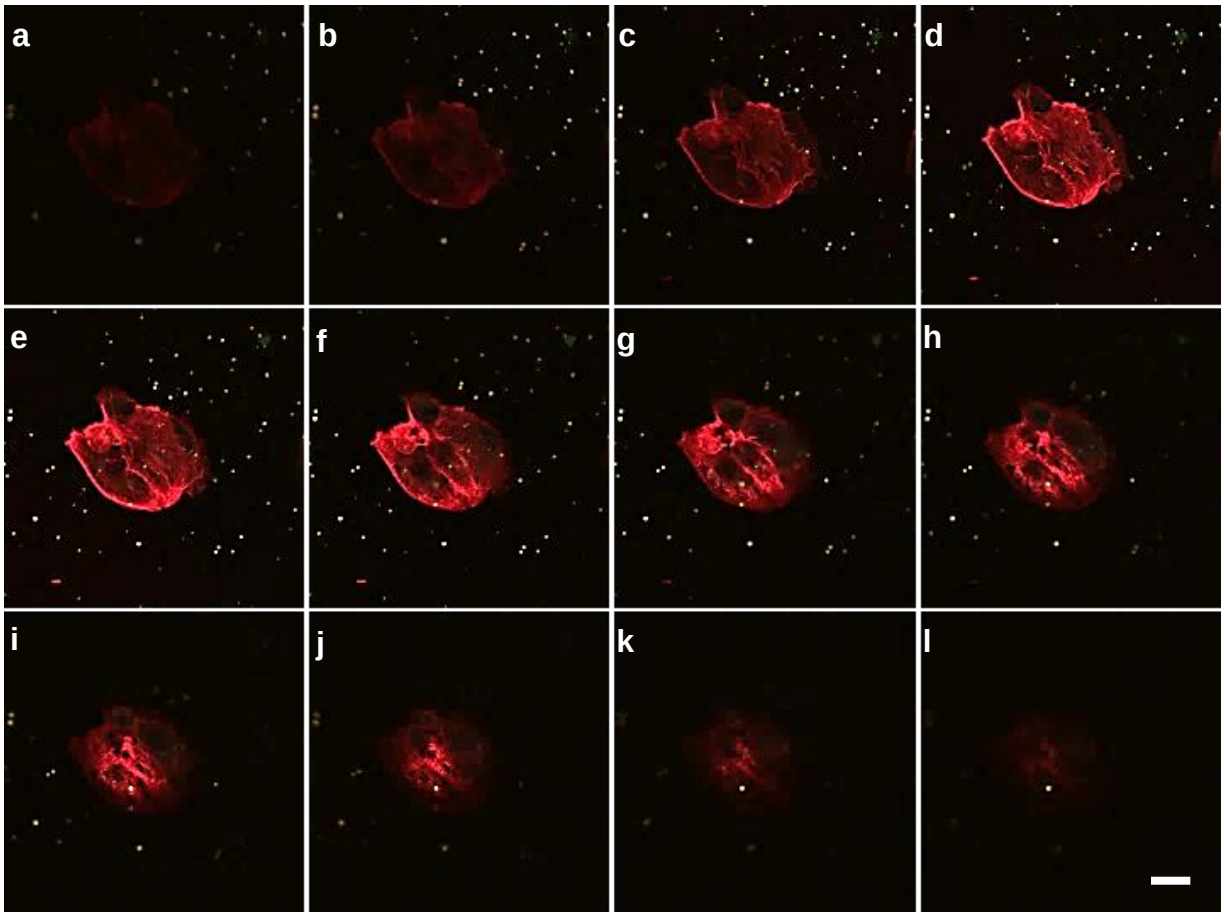

Figure 7. "Z-stack" images in confocal laser scanning microscopy analysis of a MG63 osteoblast cell (red) incubated for 24 h at 37°C, under 5% of CO_2 in DMEM supplemented with 10% of FCS, with PLGA particles (orange). "Z-stack" composed of 12 images labelled (a)-(i) covering a depth of 7,51 µm (each confocal plan was acquired at each 0,63µm in the Z axis). Scale bar = 20 µm.

Secondly, the same observation mode was achieved on LipoParticles with a lipid coating of DPPC/DPTAP/DPPE-PEG5000/TopFluor®-PC 7/90/2/1 molar ratio. Figure 8 shows different confocal planes obtained by "Z-stack" imaging, and SI4 provides another example. Interestingly, the PLGA signal is detectable at the same confocal planes as those for MG63 cells and the lipid coating (Figure 8, b-k), and absent on those confocal planes where the MG63 cells and lipid markers are not detectable (Figure 8, a and l). As a result, these observations strongly suggest the co-localization of PLGA particle cores of LipoParticles, lipid coating of LipoParticles, and MG63 osteoblast cells after an incubation for 24 h at 37°C in CCM.

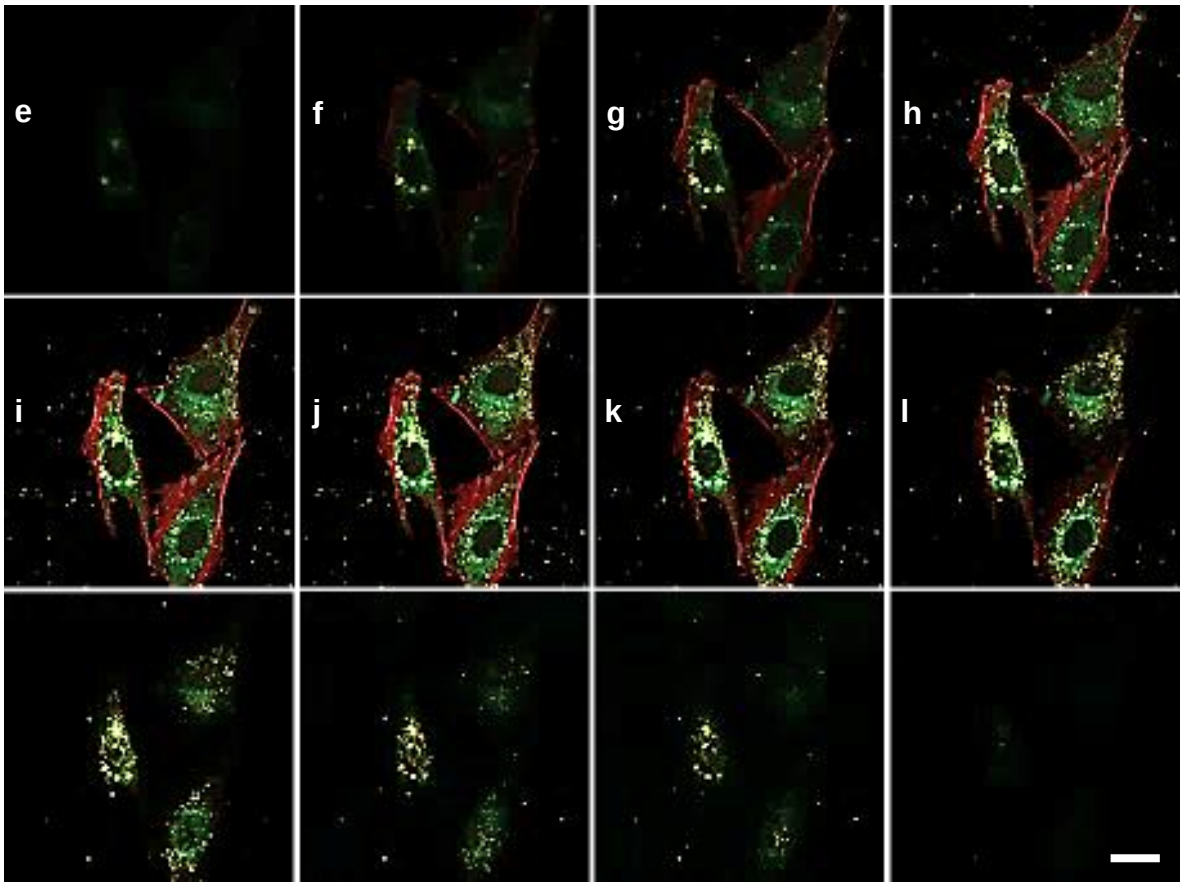

Figure 8. "Z-stack" images in confocal laser scanning microscopy analysis of MG63 osteoblast cells (red) incubated for 24 h at 37°C, under 5% of CO_2 in DMEM supplemented with 10% of FCS, with LipoParticles with a lipid coating of DPPC/DPTAP/DPPE-PEG5000/TopFluor®-PC 7/90/2/1 molar ratio (green), and with a PLGA particle core

(orange). “Z-stack” composed of 20 images (12 representative images have been selected for this figure) covering a depth of 7,63 µm (each confocal plan was acquired at each 0,40 µm in the Z axis). Another example is provided in SI4. Another example is provided in SI4.Scale bar = 50 µm.

To conclude, the analysis by confocal laser scanning microscopy allowed to prove that the lipid membrane at the surface of PLGA particles favors their internalization inside the MG63 osteoblast cells with an incubation of 3,000 LipoParticles per MG63 osteoblast cell (and with a total number of osteoblasts = 40,000). Indeed, this lipid membrane seems to play an important role for this internalization since in its absence, the PLGA particles do not penetrate inside osteoblast cells (for an average number of 3,000 PLGA particles per MG63 osteoblast cell). However, since these observations were only qualitative, as we mentioned earlier, we decided to quantify particle internalization by flow cytometry.

Evidence of an enhanced osteoblast cell internalization of LipoParticles by flow cytometry assays

In order to quantify the internalization of different assemblies inside MG63 osteoblast cells, studies in flow cytometry were realized. The flow cytometry is a qualitative and quantitative characterization technique performed on cells in suspension in a liquid. As for confocal laser scanning microcopy, the specific fluorescent staining agents were used (TopFluor®-PC to identify the lipid membranes, and rhodamine B for the PLGA particles). Besides, to confirm that the assemblies are not cytotoxic (as previously proven by WST-1 assays), we studied the viability of MG63 cells after incubation with them. Table 4 (first column) shows that the percentages of alive MG63 osteoblast cells after an incubation for 24 h at 37°C are always

above 87%, whatever the nature of assemblies. These high percentages demonstrate the validity of the experiment, the analysis method, and the results obtained by WST-1 assays.

Concerning the flow cytometry investigation, a number of "individual live cells" events of 20,000, and 22,000 liposomes or LipoParticles per MG63 osteoblast cell, were chosen. As for the confocal laser scanning microscopy analyses, the conditions of incubation of MG63 osteoblast cells with different types of colloids were 24 h at 37°C in DMEM CCM supplemented with 10% FCS. We also studied the influence of the presence of lipid-PEG conjugates in the lipid membrane of liposomes and LipoParticles. Table 4 displays the median fluorescence intensities of TopFluor®-PC (staining the lipid membranes) and rhodamine B (staining the PLGA particles). They reveal that the median fluorescence intensity of rhodamine B is about 4 to 5 times (*i.e.*, = 29,019/7,669 to 38,000/7,669) higher when the MG63 osteoblast cells were incubated with LipoParticles than PLGA particles (without the lipid coating). This result confirms the observations in confocal laser scanning microscopy, meaning that the presence of lipid coating promotes the internalization of PLGA particles in the MG63 osteoblast cells. Moreover, note that the internalization of the lipid membrane of LipoParticles is equivalent to the liposome one (median fluorescence intensity of TopFluor®PC: 17,429, and 14,448 in LipoParticles *versus* 19,035 and 10,418 in liposomes). Concerning the presence of DPPE-PEG5000 conjugates in the lipid membrane of LipoParticles, it seems to cause the decrease of their internalization in the MG63 osteoblast cells (median fluorescence intensities of rhodamine B: 29,019 with PEG chains *versus* 38,000 without lipid-PEG conjugates). In contrast, for liposomes, the opposite seems to be the case (median fluorescence intensities of TopFluor®-PC: 19,035 with lipid-PEG conjugates *versus* 10,418 without lipid-PEG conjugates). This could be explained by an internalization mechanism in MG63 osteoblast cells depending on the nature of assemblies (liposomes and LipoParticles).

Table 4. Viability tests, and median fluorescence intensities of TopFluor®-PC (staining the lipid membranes) and rhodamine B (staining the PLGA particles) obtained by flow cytometry on 20,000 "individual live cells" events, and an incubation of 22,000 liposomes or LipoParticles (without or with lipid-PEG conjugates) per MG63 osteoblast cell (corresponding gating strategies, dot plots, and overlay histograms obtained are presented in SI5).

Samples	% Live cells	Median fluorescence intensity	
		TopFluor®-PC	Rhodamine B
Liposomes DPPC/DPTAP/TopFluor®-PC 9/90/1 molar ratio	91.6	10,418	94
Liposomes with lipid-PEG conjugates DPPC/DPTAP/DPPE-PEG5000/TopFluor®-PC 7/90/2/1 molar ratio	90.4	19,035	113
PLGA particles	95.1	28	7,669
LipoParticles DPPC/DPTAP/TopFluor®-PC 9/90/1 molar ratio	92.5	14,448	38,000
LipoParticles with lipid-PEG conjugates DPPC/DPTAP/DPPE-PEG5000/TopFluor®-PC 7/90/2/1 molar ratio	89.7	17,429	29,019

Evidence of the internalization of LipoParticles in MG63 osteoblast cells infected by intracellular *Staphylococcus aureus* by TEM on ultrathin sections

The last study of this work concerned always the internalization of LipoParticles in MG63 osteoblast cells, but infected by intracellular *Staphylococcus aureus*. To this end, cells were incubated for 24 h with a LipoParticle suspension (22,000 per MG63 osteoblast cell).

Corresponding 100 nm-ultrathin sections (see their preparation in Experimental Section) were observed by TEM (Figure 9, other examples of images are also provided in SI6). In parallel, as references, the same preparation was performed on i) unexposed MG63 osteoblast cells non-infected by intracellular *Staphylococcus aureus* (image is presented in SI7), ii) unexposed MG63 osteoblast cells infected by intracellular *Staphylococcus aureus* (image is presented in SI8), iii) infected cells but incubated with PLGA particles (images are presented in SI9), iv) and suspensions of alone PLGA particles or LipoParticles (images are presented in SI10) without MG63 osteoblast cells. Figure 9 displays some cellular organelles (**N** = nucleus, **M** = mitochondria), intracellular *Staphylococcus aureus* (**B**), as well as DPPC/DPTAP/DPPE-PEG5000 8/90/2 (molar ratio) LipoParticles (**LP**, highlighted by red arrows). Despite the fact that these latter present an observed size above the one measured by DLS (Table 1), and they are less spherical than in conventional TEM (Figure 1), these white objects correspond well to LipoParticles since they are absent in the control images (*i.e.*, without the assemblies). These differences in size and morphology could be interpreted as artefactual modifications due to the number of steps required to perform such a technique (such as the dehydration of particles and LipoParticles in a graded series of ethanol, their embedding in an epoxy resin, as well as their final cut in ultrathin sections by the ultramicrotome). Indeed, previous TEM observations of ultrathin cross sections of LipoParticles, obtained by ultramicrotomy in similar conditions, have already shown the deformation of sectioned assemblies caused by compression during sectioning[21].

Figure 9 shows that the LipoParticles are internalized inside the human MG63 osteoblast cell line, close to intracellular bacteria. This favorable location of LipoParticles would very interestingly allow them to release their future antibacterial cargo, near the targeted bacteria. Note that the images of the reference constituted of PLGA particles (in SI9) reveal also their internalization. Nevertheless, with the TEM technique on ultrathin sections, the quantification

of the cell internalization magnitude, and the study of a cell internalization difference between LipoParticles and PLGA particles, are very tricky due to representativeness issues of images, and the limited number of observations due to the complexity of the stained ultrathin section preparation.

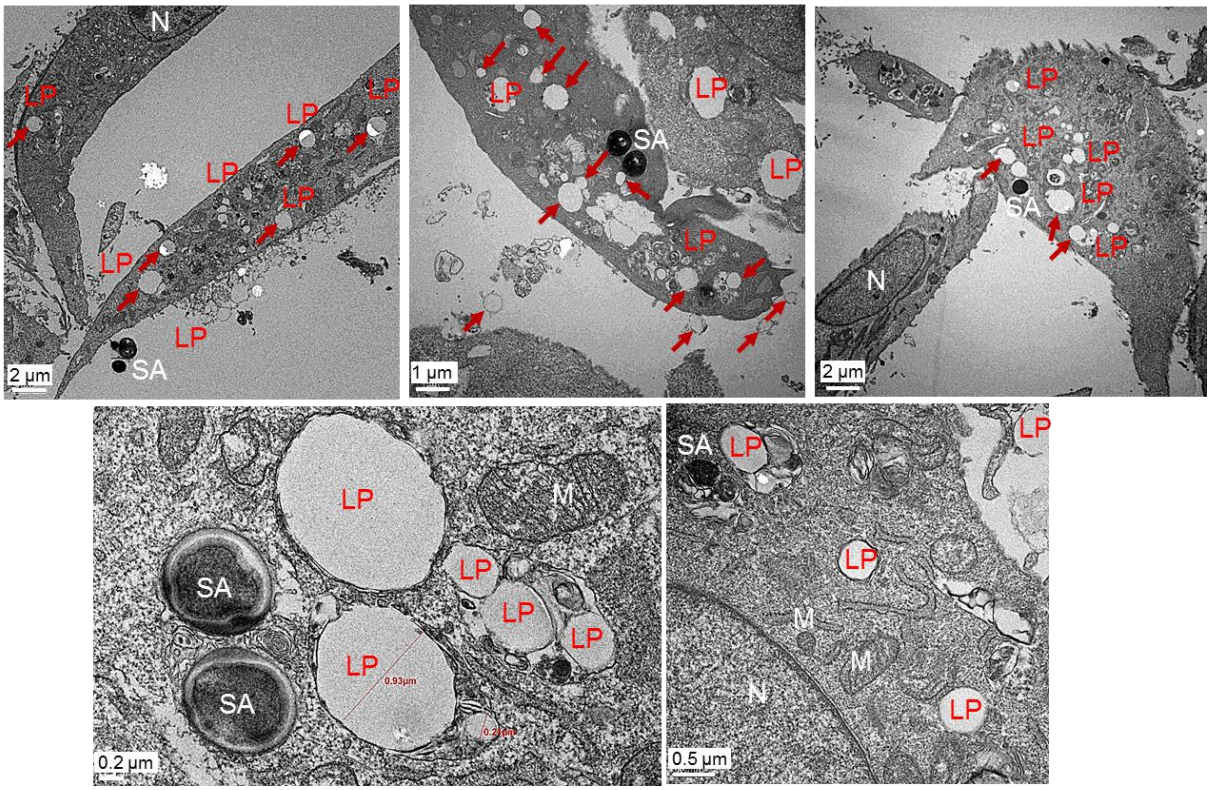

Figure 9. TEM image of ultrathin sections obtained by ultramicrotomy of MG63 osteoblast cells (**N** = nucleus, **M** = mitochondria) infected by *Staphylococcus aureus* (**SA**), incubated with LipoParticles (**LP**) composed of DPPC/DPTAP/DPPE-PEG5000 8/90/2 (molar ratio) and PLGA particles.

Conclusions

LipoParticles are core-shell assemblies, constituted of a polymer core coated by a lipid membrane, with promising perspectives in drug delivery applications. On one side, the polymer core allows the lipid coating to be stabilized, and on the other side, the lipid coating

allows the polymer core to present a biomimetic surface. In this work, the lipid modification of PLGA particles was illustrated by an inversion of zeta potential (occurring during the re-organization of cationic liposomes onto the anionic surface of polymer particles), and was shown by (cryo)-TEM (a lipid bilayer was observed onto the PLGA particles). The use of these assemblies as drug vectors is already well-reported in the literature. On the contrary, to the better of our knowledge, their capacity to go through the osteoblast cell membrane with the aim of targeting intracellular bacteria is not detailed. The study presented herein shows that the lipid coating of PLGA particles can enhance their internalization in a human osteoblast cell line (MG63) without presenting a cytotoxicity towards them for concentrations up to 1,250 $\mu g.mL^{-1}$. Moreover, this work demonstrates that these assemblies with an optimized lipid formulation (containing 2% molar of DPPE-PEG5000 conjugates) can be freeze-dried without the formation of aggregates after their re-hydration, and can be diluted 20-fold in PBS or cell culture medium without drastically modifying their size and size distribution. Finally, this study displays an intracellular localization of LipoParticles close to *Staphylococcus aureus* inside MG63 osteoblast cells leading them to be very promising candidates to carry and release antibacterial compounds close to intracellular bacteria. Further analyses to elucidate the mechanism of this osteoblast cell internalization of LipoParticles would be very interesting to even better fit the lipid formulation, the size of assemblies, and the "LipoParticle/osteoblast" number ratio.

Associated content

Supporting Information Available: Additional results including TEM images of PLGA particles, and LipoParticles **(SI1)**, Confocal laser scanning microscopy analysis of *in vitro* uptake in MG63 osteoblast cells of LipoParticles composed of DPPC/DPTAP/TopFluor®-PC

9/90/1 molar ratio **(SI2)**, Confocal laser scanning microscopy analysis of *in vitro* uptake in MG63 osteoblast cells of LipoParticles composed of DPPC/DPTAP/DPPE-PEG5000/TopFluor®-PC 7/90/2/1 molar ratio **(SI3).** "Z-stack" images in confocal laser scanning microscopy analysis of MG63 osteoblast cells incubated with LipoParticles composed of DPPC/DPTAP/DPPE-PEG5000/TopFluor®-PC 7/90/2/1 molar ratio **(SI4)**, Gating strategies, dot plots, and overlay histograms obtained by flow cytometry obtained by flow cytometry (**SI5**), TEM images of ultrathin sections (100 nm) obtained by ultramicrotomy of MG63 osteoblast cells infected by *intracellular Staphylococcus aureus* incubated with LipoParticles **(SI6)**, TEM images of ultrathin sections (100 nm) obtained by ultramicrotomy of MG63 osteoblast cells non-infected by intracellular *Staphylococcus aureus* **(SI7)**, TEM image of an ultrathin section (100 nm) obtained by ultramicrotomy of MG63 osteoblast cells infected by intracellular *Staphylococcus aureus* **(SI8)**, TEM images of ultrathin sections (100 nm) obtained by ultramicrotomy of MG63 osteoblast cells incubated with PLGA particles **(SI9)**, TEM images of ultrathin sections (100 nm) obtained by ultramicrotomy of PLGA particles, and LipoParticles composed of DPPC/DPTAP/DPPE-PEG5000 8/90/2 molar ratio **(SI10)**.

Acknowledgments. This work was financially supported by grants from the French Agence Nationale de la Recherche (ANR 2016 ANTIDOTE). The authors thank Marion Decossas (CBMN-UMR 5248, Bordeaux) for cryo-TEM observations of LipoParticles, and the scientific illustrator The Drawing Scientist (www.thedrawingscientist.com) for reviewing and optimizing the figures and graphical abstract presented in this paper.

Data availability

This research was funded, in whole or in part, by ANR # 2016 ANTIDOTE.

CRediT authorship contribution statement

Florian Vanneste: Investigation, Writing - Review & Editing, **Allison Faure:** Investigation, **Mathieu Varache:** Investigation, **Mario Menendez-Miranda:** Investigation, **Virginie Dyon-Tafani:** Investigation, **Sébastien Dussurgey:** Investigation, **Elizabeth Errazuriz-Cerda:** Investigation, **Veronica La Padula:** Investigation, **Pierre Alcouffe:** Investigation, **Marie Carrière:** Investigation**,** Supervision, Writing - Review & Editing, **Ruxandra Gref :** Conceptualization, Methodology, Supervision, Writing - Review & Editing, Funding acquisition, **Jérôme Josse :** Conceptualization, Methodology, Supervision, Writing - Review & Editing, **Frédéric Laurent :** Conceptualization, Methodology, Supervision**, Catherine Ladavière :** Conceptualization, Methodology, Supervision, Writing - Original Draft, Writing - Review & Editing, Funding acquisition

Declaration of Competing Interest

The authors declare that they have no known competing financial interests or personal relationships that could have appeared to influence the work reported in this paper.

References

1. Tande, A. J.; Patel, R., Prosthetic Joint Infection. *Clinical Microbiology Reviews* **2014,** *27* (2), 302-345.

2. Josse, J.; Velard, F.; Gangloff, S. C., Staphylococcus aureus vs. Osteoblast: Relationship and Consequences in Osteomyelitis. *Frontiers in Cellular and Infection Microbiology* **2015,** *5*, 85.

3. Marro, F. C.; Abad, L.; Blocker, A. J.; Laurent, F.; Josse, J.; Valour, F., In vitro antibiotic activity against intraosteoblastic Staphylococcus aureus: a narrative review of the literature. *The Journal of antimicrobial chemotherapy* **2021,** *76* (12), 3091-3102.

4. Shukla, R.; Peoples, A. J.; Ludwig, K. C.; Maity, S.; Derks, M. G. N.; De Benedetti, S.; Krueger, A. M.; Vermeulen, B. J. A.; Harbig, T.; Lavore, F.; Kumar, R.; Honorato, R. V.; Grein, F.; Nieselt, K.; Liu, Y.; Bonvin, A.; Baldus, M.; Kubitscheck, U.; Breukink, E.; Achorn, C.; Nitti, A.; Schwalen, C. J.; Spoering, A. L.; Ling, L. L.; Hughes, D.; Lelli, M.; Roos, W. H.; Lewis, K.; Schneider, T.; Weingarth, M., An antibiotic from an uncultured bacterium binds to an immutable target. *Cell* **2023,** *186* (19), 4059-4073.e27.

5. Patra, J. K.; Das, G.; Fraceto, L. F.; Campos, E. V. R.; Rodriguez-Torres, M. d. P.; Acosta-Torres, L. S.; Diaz-Torres, L. A.; Grillo, R.; Swamy, M. K.; Sharma, S.; Habtemariam, S.; Shin, H.-S., Nano based drug delivery systems: recent developments and future prospects. *Journal of Nanobiotechnology* **2018,** *16* (1), 71.

6. Caster, J. M.; Patel, A. N.; Zhang, T.; Wang, A., Investigational nanomedicines in 2016: a review of nanotherapeutics currently undergoing clinical trials. *Wiley interdisciplinary reviews. Nanomedicine and nanobiotechnology* **2017,** *9* e1416.

7. Ventola, C. L., Progress in Nanomedicine: Approved and Investigational Nanodrugs. *P & T : a peer-reviewed journal for formulary management* **2017,** *42* (12), 742-755.

8. Guimarães, D.; Cavaco-Paulo, A.; Nogueira, E., Design of liposomes as drug delivery system for therapeutic applications. *International Journal of Pharmaceutics* **2021,** *601*, 120571.

9. Liu, P.; Chen, G.; Zhang, J., A Review of Liposomes as a Drug Delivery System: Current Status of Approved Products, Regulatory Environments, and Future Perspectives. *Molecules* **2022,** *27* (4), 1372.

10. Large, D. E.; Abdelmessih, R. G.; Fink, E. A.; Auguste, D. T., Liposome composition in drug delivery design, synthesis, characterization, and clinical application. *Advanced Drug Delivery Reviews* **2021,** *176*, 113851.

11. Barratt, G.; Couarraze, G.; Couvreur, P.; Dubernet, C.; Fattal, E.; Gref, R.; Labarre, D.; Legrand, P.; Ponchel, G.; Vauthier, C., Polymeric Micro- and Nanoparticles as Drug Carriers. In *Polymeric Biomaterials, Revised and Expanded*, Dumitriu, S., Ed. CRC Press: 2001.

12. El-Say, K. M.; El-Sawy, H. S., Polymeric nanoparticles: Promising platform for drug delivery. *International Journal of Pharmaceutics* **2017,** *528* (1-2), 675-691.

13. Elmowafy, E. M.; Tiboni, M.; Soliman, M. E., Biocompatibility, biodegradation and biomedical applications of poly(lactic acid)/poly(lactic-co-glycolic acid) micro and nanoparticles. *Journal of Pharmaceutical Investigation* **2019**, *49*, 347-380.

14. Danhier, F.; Ansorena, E.; Silva, J. M.; Coco, R.; Le Breton, A.; Préat, V., PLGA-based nanoparticles: An overview of biomedical applications. *Journal of Controlled Release* **2012,** *161* (2), 505-522.

15. Yoo, J.; Won, Y.-Y., Phenomenology of the Initial Burst Release of Drugs from PLGA Microparticles. *ACS Biomaterials Science & Engineering* **2020,** *6* (11), 6053-6062.

16. Park, K.; Skidmore, S.; Hadar, J.; Garner, J.; Park, H.; Otte, A.; Soh, B. K.; Yoon, G.; Yu, D.; Yun, Y.; Lee, B. K.; Jiang, X.; Wang, Y., Injectable, long-acting PLGA formulations:

Analyzing PLGA and understanding microparticle formation. *Journal of Controlled Release* **2019,** *304*, 125-134.

17. Alsaab, H. O.; Alharbi, F. D.; Alhibs, A. S.; Alanazi, N. B.; Alshehri, B. Y.; Saleh, M. A.; Alshehri, F. S.; Algarni, M. A.; Almugaiteeb, T.; Uddin, M. N.; Alzhrani, R. M., PLGA-Based Nanomedicine: History of Advancement and Development in Clinical Applications of Multiple Diseases. *Pharmaceutics* **2022,** *14* (12), 2728.

18. Troutier, A.-L.; Ladavière, C., An overview of lipid membrane supported by colloidal particles. *Advances in Colloid and Interface Science* **2007,** *133* (1), 1-21.

19. Thevenot, J.; Troutier, A.-L.; David, L.; Delair, T.; Ladavière, C., Steric Stabilization of Lipid/Polymer Particle Assemblies by Poly(ethylene glycol)-Lipids. *Biomacromolecules* **2007,** *8* (11), 3651-3660.

20. Thevenot, J.; Troutier, A.-L.; Putaux, J.-L.; Delair, T.; Ladavière, C., Effect of the Polymer Nature on the Structural Organization of Lipid/Polymer Particle Assemblies. *The Journal of Physical Chemistry B* **2008,** *112* (44), 13812-13822.

21. Troutier, A.-L.; Delair, T.; Pichot, C.; Ladavière, C., Physicochemical and interfacial investigation of lipid/polymer particle assemblies. *Langmuir* **2005,** *21* (4), 1305–1313.

22. Troutier, A.-L.; Véron, L.; Delair, T.; Pichot, C.; Ladavière, C., New Insights into Self-Organization of a Model Lipid Mixture and Quantification of Its Adsorption on Spherical Polymer Particles. *Langmuir* **2005,** *21* (22), 9901-9910.

23. Bathfield, M.; Daviot, D.; D'Agosto, F.; Spitz, R.; Ladavière, C.; Charreyre, M.-T.; Delair, T., Synthesis of Lipid-α-End-Functionalized Chains by RAFT Polymerization. Stabilization of Lipid/Polymer Particle Assemblies. *Macromolecules* **2008,** *41* (22), 8346-8353.

24. Troutier-Thuilliez, A.-L.; Thevenot, J.; Delair, T.; Ladavière, C., Adsorption of plasmid DNA onto lipid/polymer particle assemblies. *Soft Matter* **2009,** *5* (23), 4739.

25. Lacour, W.; Adjili, S.; Blaising, J.; Favier, A.; Monier, K.; Mezhoud, S.; Ladavière, C.; Place, C.; Pécheur, E.-I.; Charreyre, M.-T., Far-Red Fluorescent Lipid-Polymer Probes for an Efficient Labeling of Enveloped Viruses. *Adv. Healthcare Mater.* **2016,** *5* (16), 2032-2044.

26. Bugnicourt, L.; Ladavière, C., A close collaboration of chitosan with lipid colloidal carriers for drug delivery applications. *Journal of Controlled Release* **2017,** *256*, 121-140.

27. Bugnicourt, L.; Peers, S.; Dalverny, C.; Ladavière, C., Tunable morphology of lipid/chitosan particle assemblies. *Journal of Colloid and Interface Science* **2019,** *534*, 105-109.

28. Provost, A.; Rousset, C.; Bourdon, L.; Mezhoud, S.; Reungoat, E.; Fourneaux, C.; Bresson, T.; Pauly, M.; Béard, N.; Possi-Tchouanlong, L.; Grigorov, B.; Bouvet, P.; Diaz, J.-J.; Chamot, C.; Pécheur, E.-I.; Ladavière, C.; Charreyre, M.-T.; Favier, A.; Place, C.; Monier, K., Innovative particle standards and long-lived imaging for 2D and 3D dSTORM. *Scientific reports* **2019,** *9*, 17967

29. Ayad, C.; Libeau, P.; Lacroix-Gimon, C.; Ladavière, C.; Verrier, B., LipoParticles: Lipid-Coated PLA Nanoparticles Enhanced In Vitro mRNA Transfection Compared to Liposomes. *Pharmaceutics* **2021,** *13* (3), 377-395.

30. Messerschmidt, S. K. E.; Musyanovych, A.; Altvater, M.; Scheurich, P.; Pfizenmaier, K.; Landfester, K.; Kontermann, R. E., Targeted lipid-coated nanoparticles: Delivery of tumor necrosis factor-functionalized particles to tumor cells. *Journal of Controlled Release* **2009,** *137* (1), 69-77.

31. Sengupta, S.; Eavarone, D.; Capila, I.; Zhao, G.; Watson, N.; Kiziltepe, T.; Sasisekharan, R., Temporal targeting of tumour cells and neovasculature with a nanoscale delivery system. *Nature* **2005,** *436* (7050), 568-572.

32. Bershteyn, A.; Chaparro, J.; Yau, R.; Kim, M.; Reinherz, E.; Ferreira-Moita, L.; Irvine, D. J., Polymer-supported lipid shells, onions, and flowers. *Soft Matter* **2008,** *4* (9), 1787.

33. Tan, S.; Li, X.; Guo, Y.; Zhang, Z., Lipid-enveloped hybrid nanoparticles for drug delivery. *Nanoscale* **2013,** *5* (3), 860-872.

34. Persano, F.; Gigli, G.; Leporatti, S., Lipid-polymer hybrid nanoparticles in cancer therapy: current overview and future directions. *Nano Express* **2021,** *2* (1), 012006.

35. Krishnamurthy, S.; Vaiyapuri, R.; Zhang, L.; Chan, J. M., Lipid-coated polymeric nanoparticles for cancer drug delivery. *Biomaterials Science* **2015,** *3* (7), 923-936.

36. Mandal, B.; Bhattacharjee, H.; Mittal, N.; Sah, H.; Balabathula, P.; Thoma, L. A.; Wood, G. C., Core–shell-type lipid–polymer hybrid nanoparticles as a drug delivery platform. *Nanomedicine: Nanotechnology, Biology and Medicine* **2013,** *9* (4), 474-491.

37. Ma, T.; Wang, L.; TingyuanYang; Wang, D.; Ma, G.; Wang, S., PLGA–lipid liposphere as a promising platform for oral delivery of proteins. *Colloids and Surfaces B: Biointerfaces* **2014,** *117*, 512-519.

38. Öztürk Öncel, M. Ö.; Garipcan, B.; Inci, F., Biomedical Applications: Liposomes and Supported Lipid Bilayers for Diagnostics, Theranostics, Imaging, Vaccine Formulation, and Tissue Engineering. In *Biomimetic Lipid Membranes: Fundamentals, Applications, and Commercialization*, Kök, F. N.; Arslan Yildiz, A.; Inci, F., Eds. Springer International Publishing: Cham, 2019; pp 193-212.

39. Nsairat, H.; Khater, D.; Sayed, U.; Odeh, F.; Al Bawab, A.; Alshaer, W., Liposomes: structure, composition, types, and clinical applications. *Heliyon* **2022,** *8* (5), e09394.

40. Chan, J. M.; Zhang, L.; Tong, R.; Ghosh, D.; Gao, W.; Liao, G.; Yuet, K. P.; Gray, D.; Rhee, J.-W.; Cheng, J.; Golomb, G.; Libby, P.; Langer, R.; Farokhzad, O. C., Spatiotemporal

controlled delivery of nanoparticles to injured vasculature. *Proceedings of the National Academy of Sciences* **2010,** *107* (5), 2213-2218.

41. Yi, Y.; Li, Y.; Wu, H.; Jia, M.; Yang, X.; Wei, H.; Lin, J.; Wu, S.; Huang, Y.; Hou, Z.; Xie, L., Single-step assembly of polymer-lipid hybrid nanoparticles for mitomycin C delivery. *Nanoscale Research Letters* **2014,** *9* (1), 560.

42. Hitzman, C. J.; Elmquist, W. F.; Wattenberg, L. W.; Wiedmann, T. S., Development of a Respirable, Sustained Release Microcarrier for 5-Fluorouracil I: In Vitro Assessment of Liposomes, Microspheres, and Lipid Coated Nanoparticles. *Journal of Pharmaceutical Sciences* **2006,** *95* (5), 1114-1126.

43. Li, B.; Xu, H.; Li, Z.; Yao, M.; Xie, M.; Shen, H.; Shen, S.; Wang, X.; Jin, Y., Bypassing multidrug resistance in human breast cancer cells with lipid/polymer particle assemblies. *International Journal of Nanomedicine* **2012**, *7*, 187-197.

44. Li, X.; Salzano, G.; Qiu, J.; Menard, M.; Berg, K.; Theodossiou, T.; Ladavière, C.; Gref, R., Drug-Loaded Lipid-Coated Hybrid Organic-Inorganic "Stealth" Nanoparticles for Cancer Therapy. *Frontiers in Bioengineering and Biotechnology* **2020,** *8*, 1027.

45. Mornet, S.; Lambert, O.; Duguet, E.; Brisson, A., The Formation of Supported Lipid Bilayers on Silica Nanoparticles Revealed by Cryoelectron Microscopy. *Nano Letters* **2005,** *5* (2), 281-285.

46. Jadon, R. S.; Sharma, M., Docetaxel-loaded lipid-polymer hybrid nanoparticles for breast cancer therapeutics. *Journal of Drug Delivery Science and Technology* **2019,** *51*, 475-484.

47. Harush-Frenkel, O.; Rozentur, E.; Benita, S.; Altschuler, Y., Surface Charge of Nanoparticles Determines Their Endocytic and Transcytotic Pathway in Polarized MDCK Cells. *Biomacromolecules* **2008,** *9* (2), 435-443.

48. Liu, J.; Stace-Naughton, A.; Jiang, X.; Brinker, C. J., Porous Nanoparticle Supported Lipid Bilayers (Protocells) as Delivery Vehicles. *Journal of the American Chemical Society* **2009,** *131* (4), 1354-1355.

49. Shi, S. F.; Jia, J. F.; Guo, X. K.; Zhao, Y. P.; Chen, D. S.; Guo, Y. Y.; Cheng, T.; Zhang, X. L., Biocompatibility of chitosan-coated iron oxide nanoparticles with osteoblast cells. *International Journal of Nanomedicine* **2012**, 5593.

50. Corsi, K.; Chellat, F.; Yahia, L. H.; Fernandes, J. C., Mesenchymal stem cells, MG63 and HEK293 transfection using chitosan-DNA nanoparticles. *Biomaterials* **2003,** *24* (7), 1255-1264.

51. Xu, X.; Zhang, K.; Zhao, L.; Wang, D.; Bu, W.; Zheng, C.; Sun, H., Characteristics of three sizes of silica nanoparticles in the osteoblastic cell line, MC3T3-E1. *RSC Adv.* **2014,** *4* (87), 46481-46487.

52. Cenni, E.; Avnet, S.; Granchi, D.; Fotia, C.; Salerno, M.; Micieli, D.; Sarpietro, M. G.; Pignatello, R.; Castelli, F.; Baldini, N., The Effect of Poly(d,l-Lactide-co-Glycolide)-Alendronate Conjugate Nanoparticles on Human Osteoclast Precursors. *Journal of Biomaterials Science, Polymer Edition* **2012,** *ahead-of-print* (ahead-of-print), 1-16.

53. Rabinovich, M.; Somayaji, S. N.; Pillai, R.; Hudson, M. C.; Ellington, J. K.; Bosse, M.; Horton, J.; Gonsalves, K. E., Active Polymer Nanoparticles: Delivery of Antibiotics. *MRS Proceedings* **2007, 1019**, 506.

54. Wang, H.; Liu, J.; Tao, S.; Chai, G.; Wang, J.; Hu, F. Q.; Yuan, H., Tetracycline-grafted PLGA nanoparticles as bone-targeting drug delivery system. *Int J Nanomedicine* **2015,** *10*, 5671-85.

55. Bangham, A. D.; Standish, M. M.; Watkins, J. C., Diffusion of univalent ions across the lamellae of swollen phospholipids. *Journal of Molecular Biology* **1965,** *13* (1), 238-252.

56. Pancani, E.; Mathurin, J.; Bilent, S.; Bernet-Camard, M.-F.; Dazzi, A.; Deniset-Besseau, A.; Gref, R., High-Resolution Label-Free Detection of Biocompatible Polymeric Nanoparticles in Cells. *Particle & Particle Systems Characterization* **2018,** *35* (3), 1700457.

57. Bourguignon, T.; Torrano, A. A.; Houel-Renault, L.; Machelart, A.; Brodin, P.; Gref, R., An original methodology to study polymeric nanoparticle-macrophage interactions: Nanoparticle tracking analysis in cell culture media and quantification of the internalized objects. *International Journal of Pharmaceutics* **2021,** *610*, 121202.

58. Abdelwahed, W.; Degobert, G.; Stainmesse, S.; Fessi, H., Freeze-drying of nanoparticles: Formulation, process and storage considerations. *Advanced Drug Delivery Reviews* **2006,** *58* (15), 1688-1713.

59. Shulkin, P. M.; Seltzer, S. E.; Davis, M. A.; Adams, D. F., Lyophilized liposomes: a new method for long-term vesicular storage. *Journal of Microencapsulation* **1984,** *1* (1), 73-80.

60. Stark, B.; Pabst, G.; Prassl, R., Long-term stability of sterically stabilized liposomes by freezing and freeze-drying: Effects of cryoprotectants on structure. *European Journal of Pharmaceutical Sciences* **2010,** *41* (3-4), 546-555.

61. van den Hoven, J. M.; Metselaar, J. M.; Storm, G.; Beijnen, J. H.; Nuijen, B., Cyclodextrin as membrane protectant in spray-drying and freeze-drying of PEGylated liposomes. *International Journal of Pharmaceutics* **2012,** *438* (1-2), 209-216.

62. Chaudhury, A.; Das, S.; Lee, R. F. S.; Tan, K.-B.; Ng, W.-K.; Tan, R. B. H.; Chiu, G. N. C., Lyophilization of cholesterol-free PEGylated liposomes and its impact on drug loading by passive equilibration. *International Journal of Pharmaceutics* **2012,** *430* (1-2), 167-175.

63. Vega, E.; Egea, M.A.; Calpena, A.C.; Espina, M.; García, M.L., Role of hydroxypropyl-beta-cyclodextrin on freeze-dried and gamma-irradiated PLGA and

PLGA–PEG diblock copolymer nanospheres for ophthalmic flurbiprofen delivery. *International Journal of Nanomedicine* **2012**, 1357-1371.

64. Alshehri, A.; Grabowska, A.; Stolnik, S., Pathways of cellular internalisation of liposomes delivered siRNA and effects on siRNA engagement with target mRNA and silencing in cancer cells. *Scientific reports* **2018,** *8* (1), 3748.

65. Un, K.; Sakai-Kato, K.; Oshima, Y.; Kawanishi, T.; Okuda, H., Intracellular trafficking mechanism, from intracellular uptake to extracellular efflux, for phospholipid/cholesterol liposomes. *Biomaterials* **2012,** *33* (32), 8131-41.

66. Przybylo, M.; Glogocka, D.; Dobrucki, J. W.; Fraczkowska, K.; Podbielska, H.; Kopaczynska, M.; Borowik, T.; Langner, M., The cellular internalization of liposome encapsulated protoporphyrin IX by HeLa cells. *European journal of pharmaceutical sciences : official journal of the European Federation for Pharmaceutical Sciences* **2016,** *85*, 39-46.

67. Braun, T.; Kleusch, C.; Naumovska, E.; Merkel, R.; Csiszár, A., A bioanalytical assay to distinguish cellular uptake routes for liposomes. *Cytometry Part A* **2016,** *89* (3), 301-308.